JCMM
Available online at
www.jcmm.ro
www.jcmm.org

J. Cell. Mol. Med. Vol 10, No 4, 2006 pp. 960-990

Caveolae in smooth muscles: nanocontacts

L.M. Popescu [a,b]*, Mihaela Gherghiceanu [a], E. Mandache [a], D. Cretoiu [a,b]

[a] "Victor Babeº" National Institute of Pathology, Bucharest, Romania
[b] Department of Cellular and Molecular Medicine, "Carol Davila" University of Medicine and Pharmacy, Bucharest, Romania

Received: August 15, 2006; Accepted: November 2, 2006

Abstract

Smooth muscle cell (SMC) caveolae have been investigated by quantitative and qualitative analysis of transmission electron microscopy (TEM) images of rat stomach, bladder and myometrium, guinea pig taenia coli, human ileum, and rat aortic SMCs. Ultrathin (below 30 nm) serial sections were used for examination of caveolar morphology and their connections with SMC organelles. Average caveolar diameter was smaller in vascular SMCs (70 nm, n=50) than in visceral SMCs (77 nm, n=100), but with the same morphology. Most of the caveolae, featured as flask-shaped plasma membrane (PM) invaginations, opened to the extracellular space through a 20 nm *stoma* (21 ± 3nm) having a 7 nm thick *diaphragm*. A small percentage of caveolae (3%), gathered as grape-like clusters, did not open directly to the extracellular space, but to irregular PM pockets having a 20-30 nm opening to the extracellular space. In visceral SMCs, caveolae were disposed in 4 - 6 rows, parallel to myofilaments, whilst aortic SMCs caveolae were arranged as clusters. This caveolar organization in rows or clusters minimizes the occupied volume, providing more space for the contractile machinery. The morphometric analysis of relative volumes (% of cell volume) showed that caveolae were more conspicuous in visceral than in vascular SMCs (myometrium - 2.40%; bladder - 3.66%, stomach - 2.61%, aorta - 1.43%). We also observed a higher number of caveolae per length unit of cell membrane in most visceral SMCs compared to vascular SMCs (myometrium - 1.06/µm, bladder - 0.74/µm, aorta - 0.57/µm, stomach - 0.48/µm). Caveolae increase the cellular perimeter up to 15% and enlarge the surface area of the plasma membrane about 80% in SMCs. Three-dimensional reconstructions (15μ^3) showed that most caveolae, in both visceral and vascular SMCs, have nanocontacts with SR (87%), or with mitochondria (10%), and only 3%, apparently, have no contact with these organelles. Usually, 15 nm wide *junctional spaces* exist between caveolae and SR, some of them with nanostructural links between each other or with mitochondria: direct contacts (space < 2 nm or *none*) and molecular links, so called 'feet' (about 12 nm electron dense structures between organellar membranes). Direct contacts possibly allow molecular translocation between the two membranes. Electron-dense 'feet'-like structures suggest a molecular link between these organelles responsible for intracellular Ca^{2+} homeostasis (*excitation-contraction coupling* or *pharmaco-mechanical coupling*). Close appositions (~15 nm) have also been observed between caveolae and perinuclear SR cisterna, suggesting that caveolae might be directly implicated in *excitation-transcription coupling*.

Keywords: caveolae • smooth muscle cells • sarcoplasmic reticulum • mitochondria • nanocontacts • Ca^{2+} homeostasis • excitation-contraction coupling • excitation-transcription coupling • 3D reconstruction • nuclear envelope

Introduction

One of the most striking ultrastructural features of the smooth muscle cells (SMC) is the ordered strands of caveolae on their surface. Caveolae are flask- or Ω-shaped (Fig. 1) plasmalemmal nanodomains and their structural identity was discovered 50 years ago by transmission electron microscopy [1, 2]. Caveolae seem to be steady-state plasma membrane domains with a lipid and protein composition favoring many different functions [reviews: 3–14]. It was supposed

* Correspondence to: L.M. POPESCU, M.D., Ph.D.
Department of Cellular and Molecular Medicine,
"Carol Davila" University of Medicine and Pharmacy,
P.O. Box 35-29, Bucharest 35, Romania.
E-mail: LMP@jcmm.org

doi:10.2755/jcmm010.004.17

that caveolae are specialized lipid rafts (*e.g.* [15, 16]), but the existence of lipid rafts seems elusive or even illusive [17]. Caveolar structural assembly depends on cholesterol, sphingolipids and a family of integral membrane proteins named caveolins [18]. SMC caveolae could be involved in a large number of physiological events, such as: potocytosis [19], endocytosis [20], signal transduction [10, 11, 13, 14, 21], mechanotransduction [22, 23], cholesterol trafficking [24, 25], control of cellular growth and proliferation [26] etc. However, SMC caveolae seem essentially implicated in calcium handling: excitation-contraction coupling, pharmaco-mechanical coupling, excitation-transcription coupling [4, 11, 13, 14, 21, 27–35].

In the postgenomic era, much interest is focused on the spatial relationships between organelles, including membrane microdomains, as well as macromolecular pathways followed by signaling ions and molecules. Obviously, the ultrastructural and nanostructural relationships between SMC caveolae and organelles are not yet fully acknowledged. Although this interaction was supposed and partially documented by classical electronmicroscopy and ultrastructural cytochemistry [21, 27–29, 36, 37], the only recent attractive finding seems to be the existence of the so-called 'Ca^{2+} release units' suggested by Franzini-Armstrong's group [38], by analogy with skeletal and cardiac muscles [39]. Indeed, we identified such 'Ca^{2+} release units' in human myometrium [40] and fallopian tube [41] smooth muscle.

We previously reported that strategic nanoscale assemblies formed by caveolae-SR or caveolae-mitochondria exist in the cortical cytoplasm of SMC [35]. These complexes could be responsible for a vectorial control of free Ca^{2+} cytoplasmic concentrations in definite nanospaces and for selective activation of specific Ca^{2+} signaling pathways.

The aim of this study is to present quantitative data about caveolae of visceral and vascular SMC, particularly the connections and nanocontacts with SR and mitochondria, but also with the *nuclear envelope*.

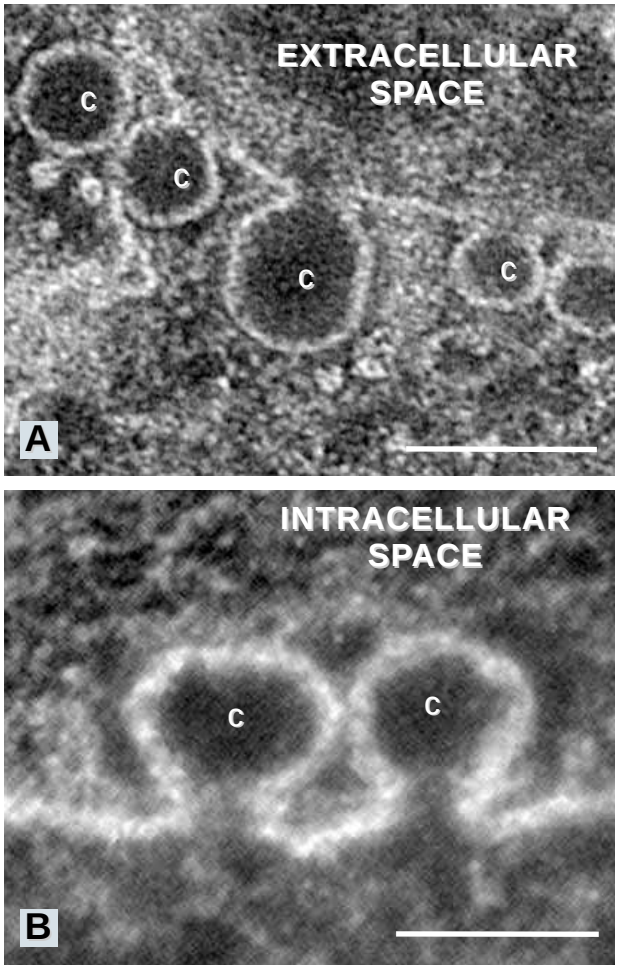

Fig. 1. TEM negative images emphasize the emblematic flask-shape (**A**) or Ω - shape (**B**) of the caveolae (c). SMC of rat bladder. Scale bar, 100nm.

Material and methods

Material

Female Wistar rats and guinea pigs were used for ultrastructural study of visceral and vascular smooth muscle cells. Rats of 200g body weight had free access to food and water and were maintained in temperature-controlled rooms with a 12h light/dark cycle. All animal experiments were carried out in accordance with the international Guidelines for Animal Experimentation. All procedures were performed under anesthesia with sodium pentobarbital (100 mg/kg body weight). The smooth muscles were taken from myometrium, bladder, stomach, taenia coli and aorta for the study of caveolae, SR, and mitochondria. Fixation was performed by perfusion through the heart with a mixture of 4% paraformaldehyde and 1% glutaraldehyde in 0.1 M phosphate buffer (pH 7.4). Smooth muscle fragments from normal portion of human ileum (surgically removed for a tumoral process) were also used.

Transmission electron microscopy (TEM)

Tissue samples of about 1mm^3 were supplementary fixed by immersion in 4% glutaraldehyde in 0.1M cacodylate buffer, pH 7.4 at 4^{o}C, for 4h. Samples were post-fixed in 1%OsO_4 and 1.5% $K_4Fe(CN)_6$ (potassium ferrocyanide-reduced osmium), in 0.1M cacodylate buffer at room temperature for 1h. This method was used because caveolae and SR are not easily visible at relatively low magnifications, by using only OsO_4 postfixation (Fig. 2). Samples were further dehydrated in increased graded ethanols followed by propylene oxide and were embedded in Epon 812 at 60^{o}C, for 48h.

Thin sections were stained with 1% uranyl acetate and Reynolds's lead citrate. Usually the ultrathin sections were cut at 60-80 nm but for short series (<10 sections) the ultrathin sections were cut at 35 or 30 nm thickness setting on the ultramicrotome stage. The examination has been performed with a Philips 301 or CM 12 Philips transmission electron microscope at 60kV.

The few ultrastructural images of the subcellular localization of Ca^{2+}-storage/release sites in smooth muscles (SR, mitochondria, nuclear envelope) presented here, were obtained by precipitation with oxalate, as described previously [27, 28], and such preparations were *not* stained (contrasted).

3D reconstruction

Three-dimensional (3D) spatial relationships between caveolae and organelles were studied for 1μm^3 volume stomach SMC reconstruction, 10 μm^3 volume in urinary bladder SMC and 2.5 μm^3 volume in myometrium. Serial electron photomicrographs (negatives) were digitized at 1200 dpi by scanning. The images were imported as tiff documents on the **'***Reconstruct'* software (Reconstruct 1078, 1996-2006 John C. Fiala; *http://synapses.bu.edu*) [42]. The images were calibrated by drawing traces on an image of a known size scale. Section thickness was set at 0.035 μm for reconstruction in stomach and bladder and at 0.030 μm for reconstruction in myometrium and human ileum. The Reconstruct software was used for alignment of images with the respect to the specific structures of interest: caveolae, peripheral sarcoplasmic reticulum, and peripheral mitochondria. The 3D reconstructions and measurements were performed on the outlines drawn contours on the specific cellular structures. Contours of the same structure from different serial sections were arranged into object using the Reconstruct software.

Serial ultrathin aligned sections and computer–aided tracing of profiles on sections were followed by automatic 3D surface generation and rendering. For the cell membranes we selected reconstruction as *traces*, and for the mitochondria and SR 3D representation we chose a *Boissonnat surface*. For caveolar 3D representation we used 3D substitution as a *sphere* of the contours traced only in a single section of 30 nm thicknesses. Some caveolae could be seen in two serial sections but were traced only on the section in which they had the largest diameter. All reconstructed images presented in this paper were saved from the 3D scene.

Quantitative analysis

Organelle relative volumes were obtained using a point-counting morphometric approach [43]. Low magnifications (9,100x) were used for evaluation of the cell, extra-

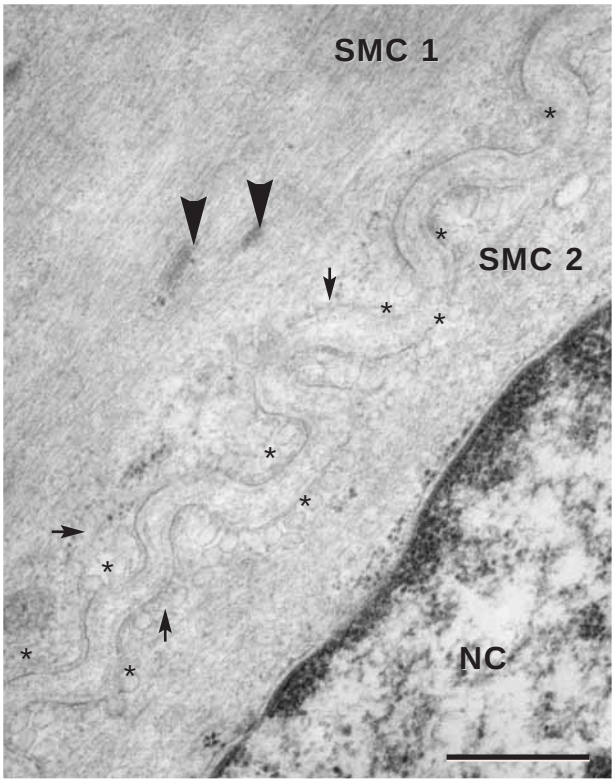

Fig 2. The sarcolemma of SMC possesses specialized nanodomains - caveolae. More than 20 caveolae (*) and peripheral SR cisternae (arrow) are barely visible in the crowded cytoplasm of the SMC in routine TEM specimens (OsO_4 only). Dense bodies - arrowheads. Two SMC from *taenia coli*. NC-nucleus. Scale bar = 0.5 μm.

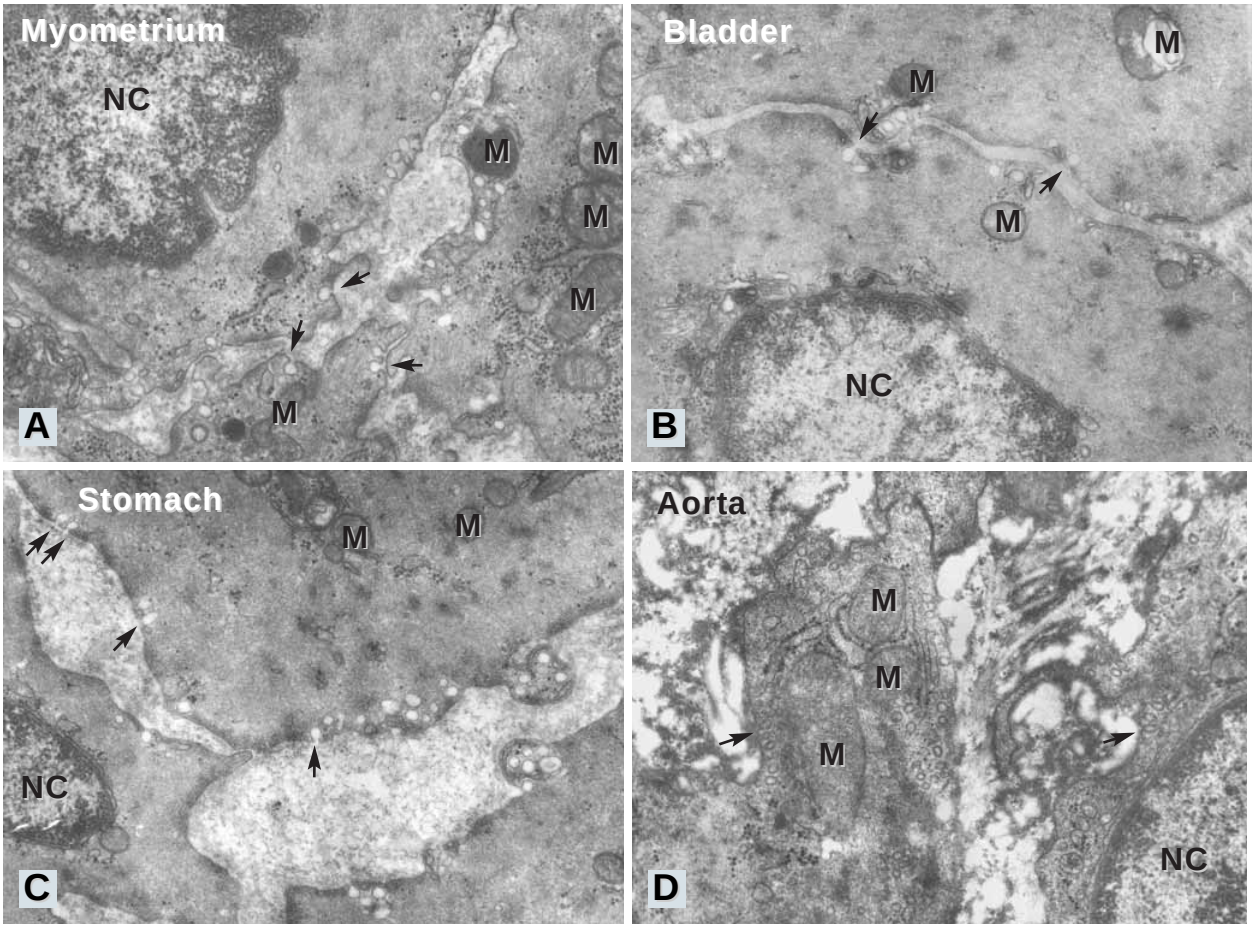

Fig. 3. Low-magnification electron micrographs of cross-sectioned smooth muscle cells from the rat *myometrum* (**A**), *bladder* (**B**), *stomach muscularis mucosae* (**C**) and *aorta* (**D**) showing that peripheral SR and mitochondria are exclusively located in the caveolar domains. Caveolae visibly opened to the extracellular space - arrows, M - mitochondria, NC - nucleus. *En block* staining tissues with potassium ferrocyanide-reduced osmium tetroxide made easier visible the sarcoplasmic reticulum elements and caveolae. ME x19,000.

cellular space and mitochondria and higher magnifications (38,000x) for the contribution of mitochondria, caveolae, and endoplasmic reticulum. The volume fractions of the cell organelles were calculated from the ratios of caveolae/mitochondria, central SR/mitochondria and peripheral SR/mitochondria as well as mitochondria/cell, after subtraction of the extracellular space. Relative volumes were also calculated for complexes formed by caveolae + peripheral SR, and complexes formed by caveolae, peripheral SR ± mitochondria as complex/cell ratio. *Mitochondria and smooth endoplasmic reticulum (SR) were considered peripheral if their membranes were located less than 150 nm distance from the sarcolemma*. Data represent mean ± SD. The areas occupied by clusters of caveolae or SR ± mitochondria were measured using the National Institutes of Health ImageJ software. The distances between different organelles or electron-dense structures were also measured with NIH ImageJ. The number of caveolae/μm was measured with a chartometer on images at 30,400x magnification.

Results and discussion

Macrodomains of smooth muscle cells

The plasma membrane of smooth muscle cells has two structural macrodomains: a caveolae-rich domain and an electron-dense caveolae-free domain (the so called ‘dense plaques’, anchoring

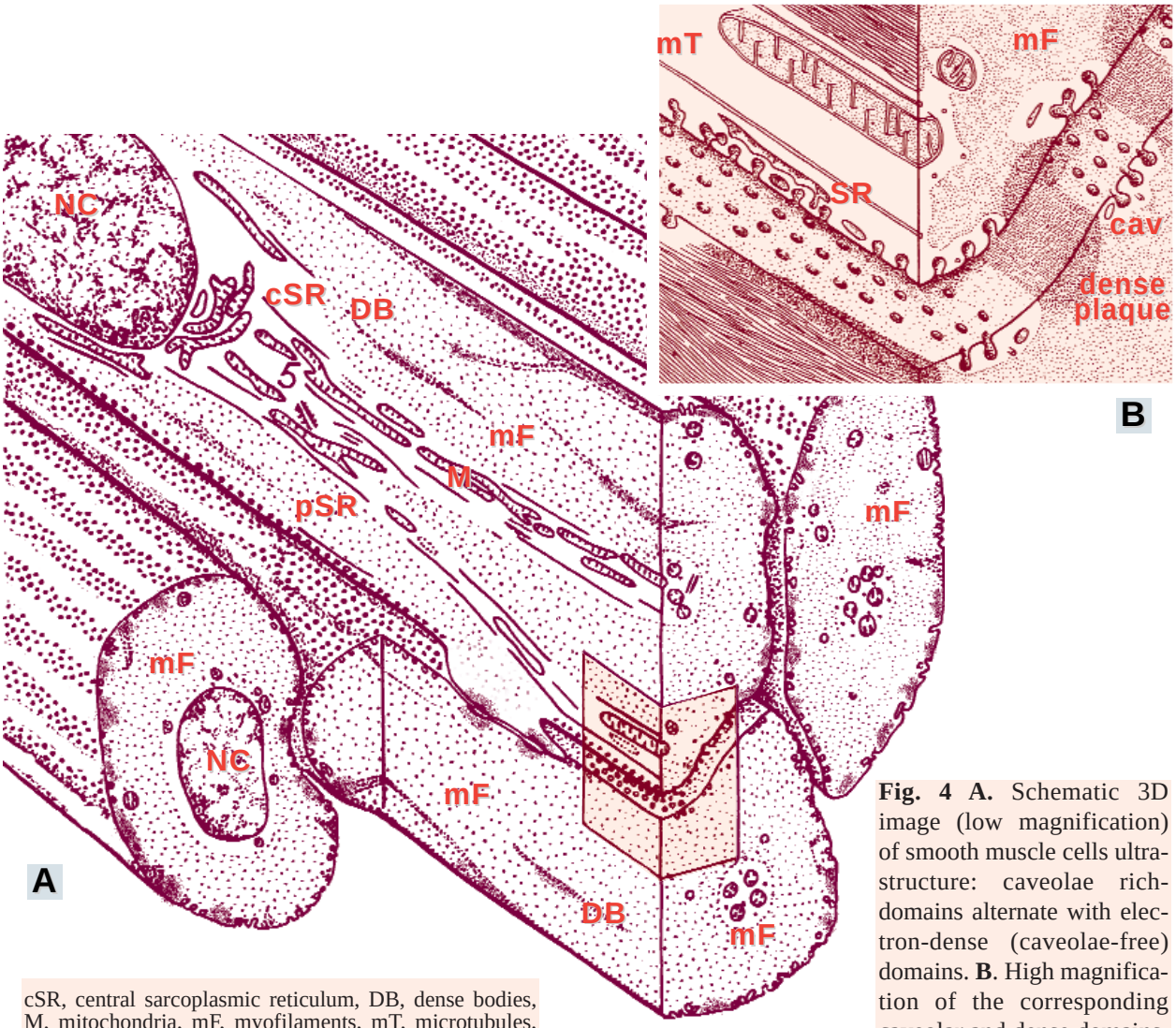

cSR, central sarcoplasmic reticulum, DB, dense bodies, M, mitochondria, mF, myofilaments, mT, microtubules, NC, nucleus, pSR, peripheral sarcoplasmic reticulum

Fig. 4 A. Schematic 3D image (low magnification) of smooth muscle cells ultrastructure: caveolae rich-domains alternate with electron-dense (caveolae-free) domains. **B**. High magnification of the corresponding caveolar and dense domains.

sites for myofilaments, composed of a complex of proteins like: vinculin, paxillin, talin...) (Fig. 3–6). The electron-dense bands alternate with bands of PM containing caveolae. Both of them are 0.3–0.5 µm equally wide and run parallel with the long axis of the SMC (Fig. 4, 5A).

The morphometric analysis revealed different relative volumes occupied by caveolae in different types of SMC (Table 1). The relative volumes showed that caveolae are most conspicuous in visceral SMC than in vascular SMC (myometrium - 2.40%; bladder - 3.66%, stomach - 2.61% and aorta - 1.43%). This is in full agreement with the data we previously reported [27], for SMC of guinea pig *taenia coli*: 3.5±0.3%, and about 3% for intestinal smooth muscle [21]. The number of caveolae per length of cell membrane was also different (Table 2). A higher number of caveolae per length unit was found in visceral compared to vascular SMC (myometrium - 1.06/µm, bladder - 0.74/µm, aorta - 0.57/µm) except the SMC from *muscularis mucosae* of stomach (0.48/µm). Usually, caveolae appear in groups of 2–5 but sometimes more that 30 caveolae could be seen in one row in visceral SMC (Fig. 3, 5).

Distribution of caveolae

In TEM sections parallel to the plasma membrane, caveolae appear as groups of 4–6 linear rows, ori-

Table 1. Average relative volumes (% of cellular volume) of organelles in smooth muscle cells of Wistar rat *.

SMC	Extra CELLULAR	CELLULAR										
		NC	cytoplasm	MITO	rER	central SR	peripheral SR	Golgi	Dense bodies	CAV	SR-CAV complexes	SR-CAV-MITO complexes
stomach	20.3%	14.7%	72.8%	2.8%	0.1%	0.5%	5.0%	0.03%	2.4%	2.6%	3.1%	3.2%
bladder	8.4%	9.8%	78.0%	2.6%	0.4%	0.2%	4.0%	0.02%	3.3%	3.7%	4.2%	3.7%
myometrium	12.8%	25.1%	74.9%	5.6%	1.2%	1.6%	2.1%	0.10%	2.4%	2.4%	1.8%	1.9%
aorta	17.4%	29.2%	58.3%	2.8%	0.5%	1.0%	5.8%	0.20%	1.2%	1.4%	2.0%	1.3%

CAV-caveolae, S-sarcoplasmic reticulum, rE-rough endoplasmic reticulum, MITO-mitochondria, NC-nucleus.

* We reported previously [27], in an almost complete morphometric study of SMC from guinea pig *taenia coli* the following average volumes: nucleus, 12.9±1.1; perinuclear cisterna - 0.3±0.05%; mitochondria 4.7±0.4%; SR - 2.4±0.2%.

Table 2. Average number of caveolae per length unit of membrane in smooth muscle cells of Wistar rat.

Wistar rat tissue	caveolae/ µm	estimated nr. of caveolae/ µm^2	estimated nr. of caveolae/ µm^3
stomach muscularis mucosa [115 caveolae /237 µm]	0.48	0.69	13.88
bladder [368 caveolae /498 µm]	0.74	0.41	8.35
myometrium [210 caveolae /197 µm]	1.06	0.70	14
aorta [170 caveolae /296 µm]	0.57	0.39	7.87

ented along the axis of the muscle fiber. This distribution is noticeable in the stretched SMC (Fig. 5A). Generally, SMC have a more irregular shape in aorta and caveolae seem to be disposed in clusters (Fig. 3D). The caveolae appear to have an ordered position in rows (Fig. 5A). Moreover, we observed (on tangential sections) that the centers of adjacent caveolae are situated at the shorter possible distance (Fig. 7–9). Therefore, we assume that caveolae adopt this spatial assembly in order to offer a larger space to the contractile machinery in SMC (Fig. 6). The distances among caveolae were from 2 to 20 nm, possibly dependening on contraction or relaxation state of the SMC (Fig. 8, 9), and, eventually, the type of contraction: isotonic or isometric.

Ultrastructure of caveolae

Caveolae have been described as flask-shaped or Ω -shaped plasma membrane (in)foldings (Fig. 1). Caveolae of visceral SMC had an average diameter of 77 nm (100 caveolae measured: 77.67 ± 12.3 nm) but most of them fluctuate between 65 and 75 nm

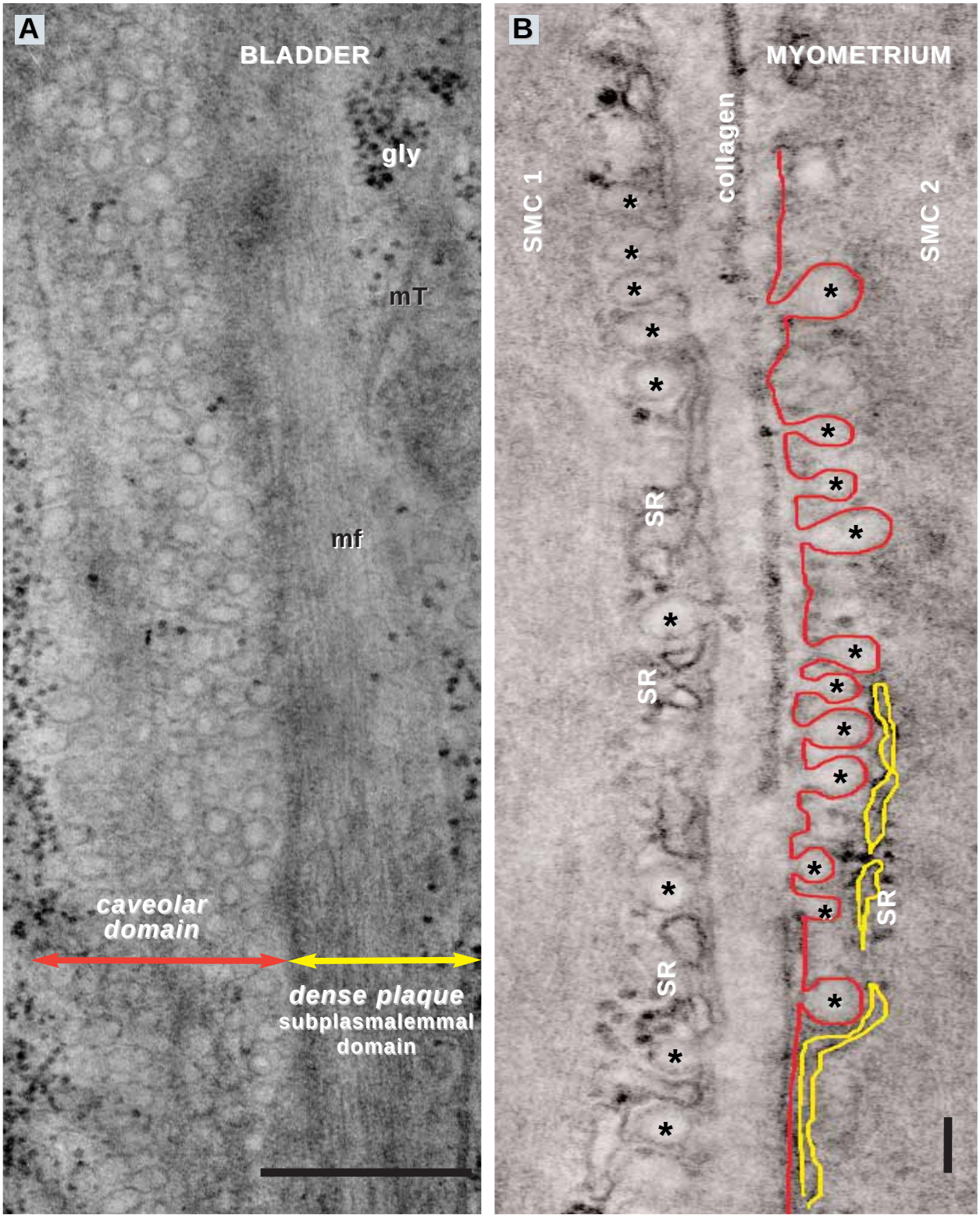

Fig. 5 A. TEM image just beneath plasma membrane shows characteristic domains of the SMC. Caveolar domains alternate with dense plaques domains and run parallel with long axis of SMC. Caveolae are organized in linear arrays. SMC from *rat bladder*. mT - microtubule; mf - myofilaments; gly - glycogen. Scale bar = 0.5 μm. **B.** Caveolar domains facing each other in two neighboring SMC from *rat myometrum*. Caveolae (*; red line in SMC2) are in close proximity with tubules of the peripheral sarcoplasmic reticulum (SR; yellow lines in SMC2). Scale bar = 100nm.

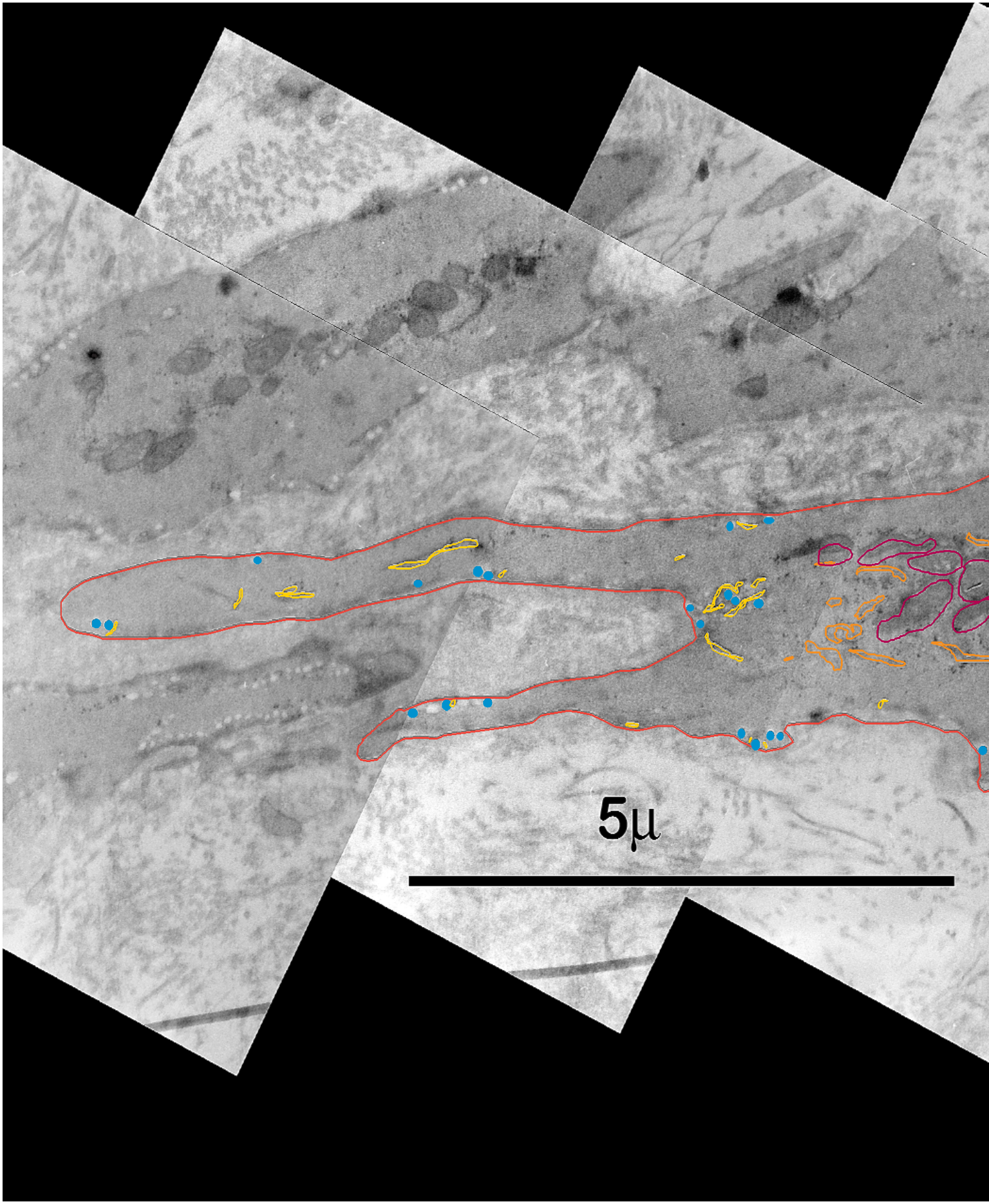
5μ

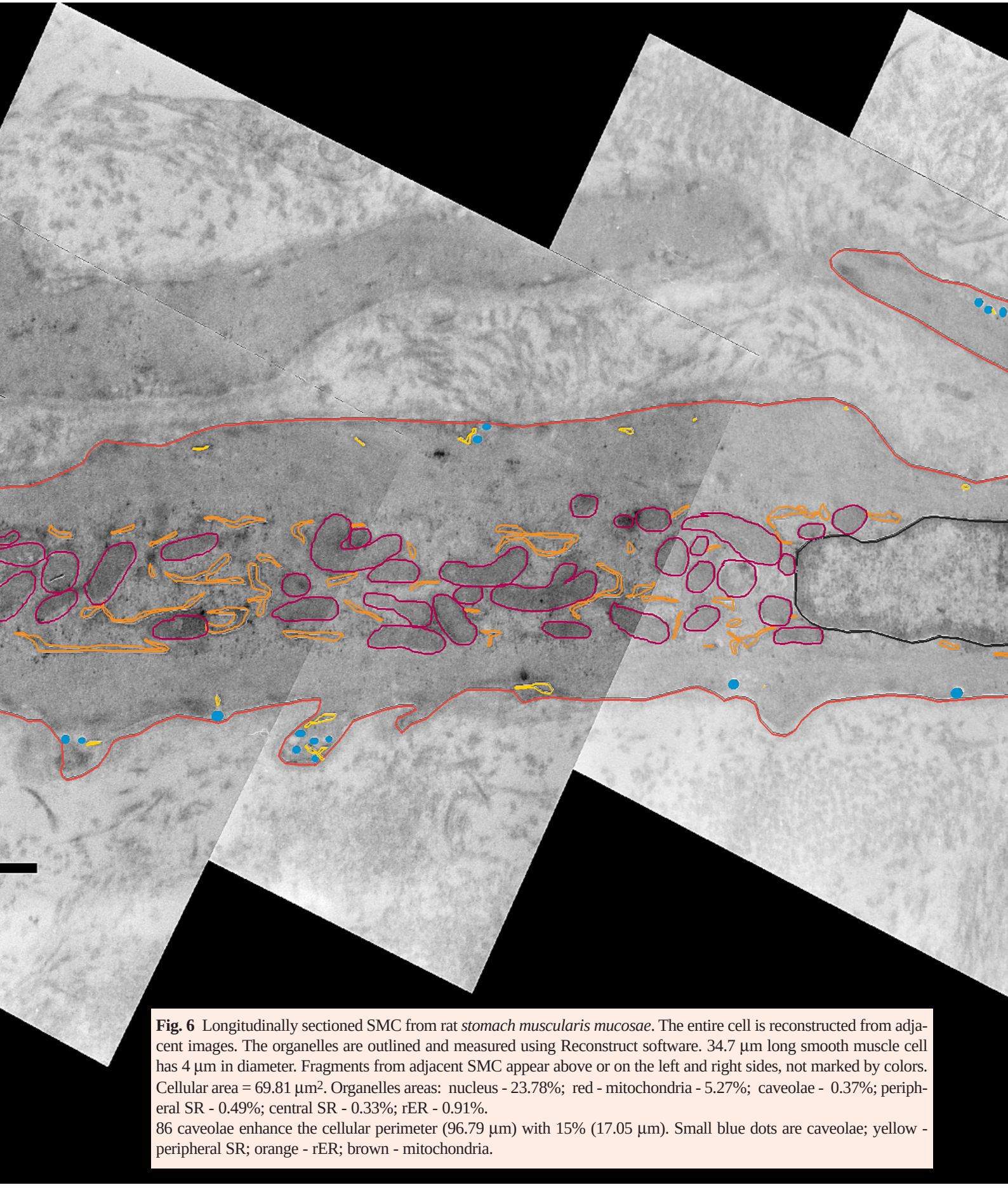

Fig. 6 Longitudinally sectioned SMC from rat *stomach muscularis mucosae*. The entire cell is reconstructed from adjacent images. The organelles are outlined and measured using Reconstruct software. 34.7 μm long smooth muscle cell has 4 μm in diameter. Fragments from adjacent SMC appear above or on the left and right sides, not marked by colors. Cellular area = 69.81 μm^2. Organelles areas: nucleus - 23.78%; red - mitochondria - 5.27%; caveolae - 0.37%; peripheral SR - 0.49%; central SR - 0.33%; rER - 0.91%.
86 caveolae enhance the cellular perimeter (96.79 μm) with 15% (17.05 μm). Small blue dots are caveolae; yellow - peripheral SR; orange - rER; brown - mitochondria.

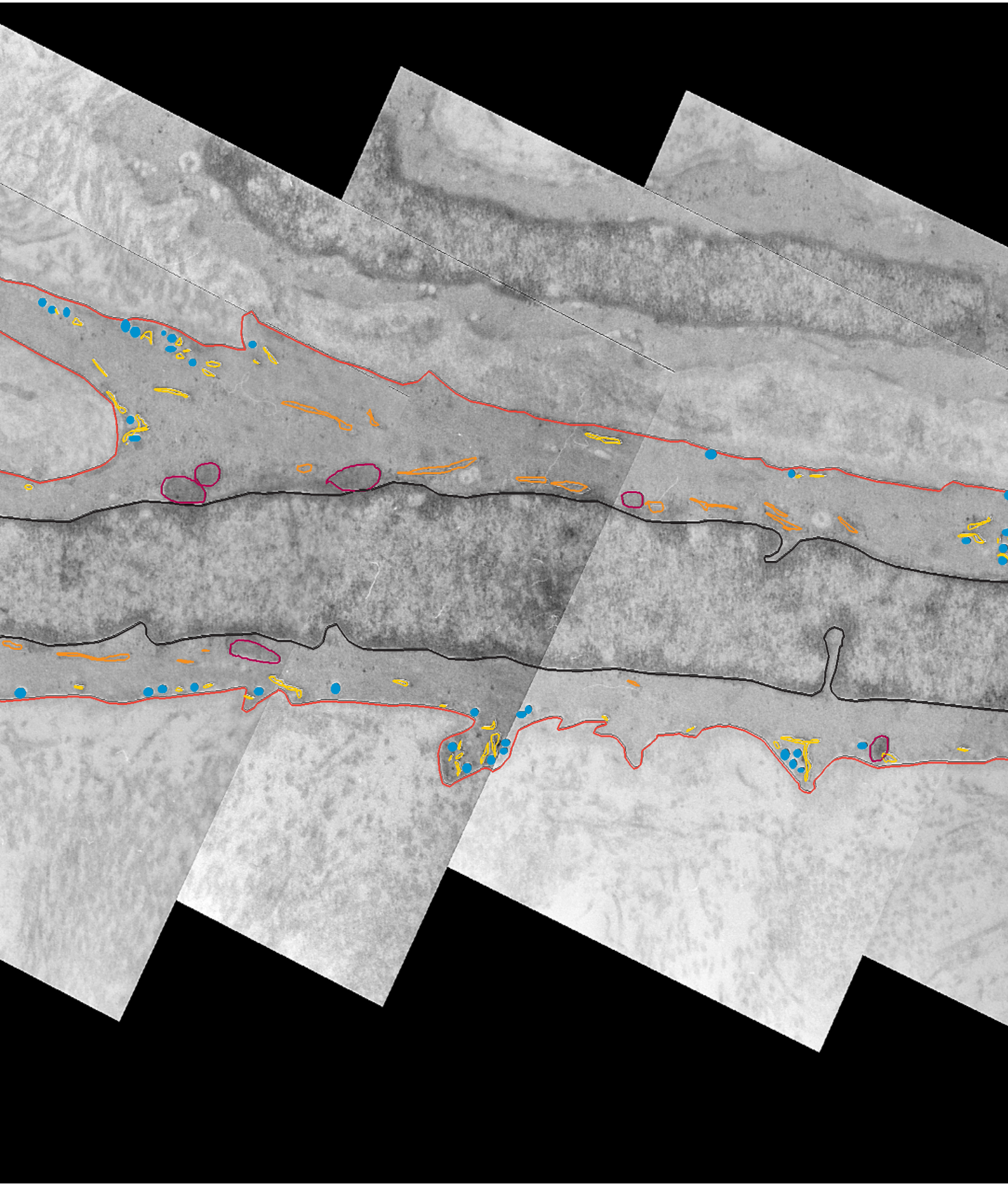

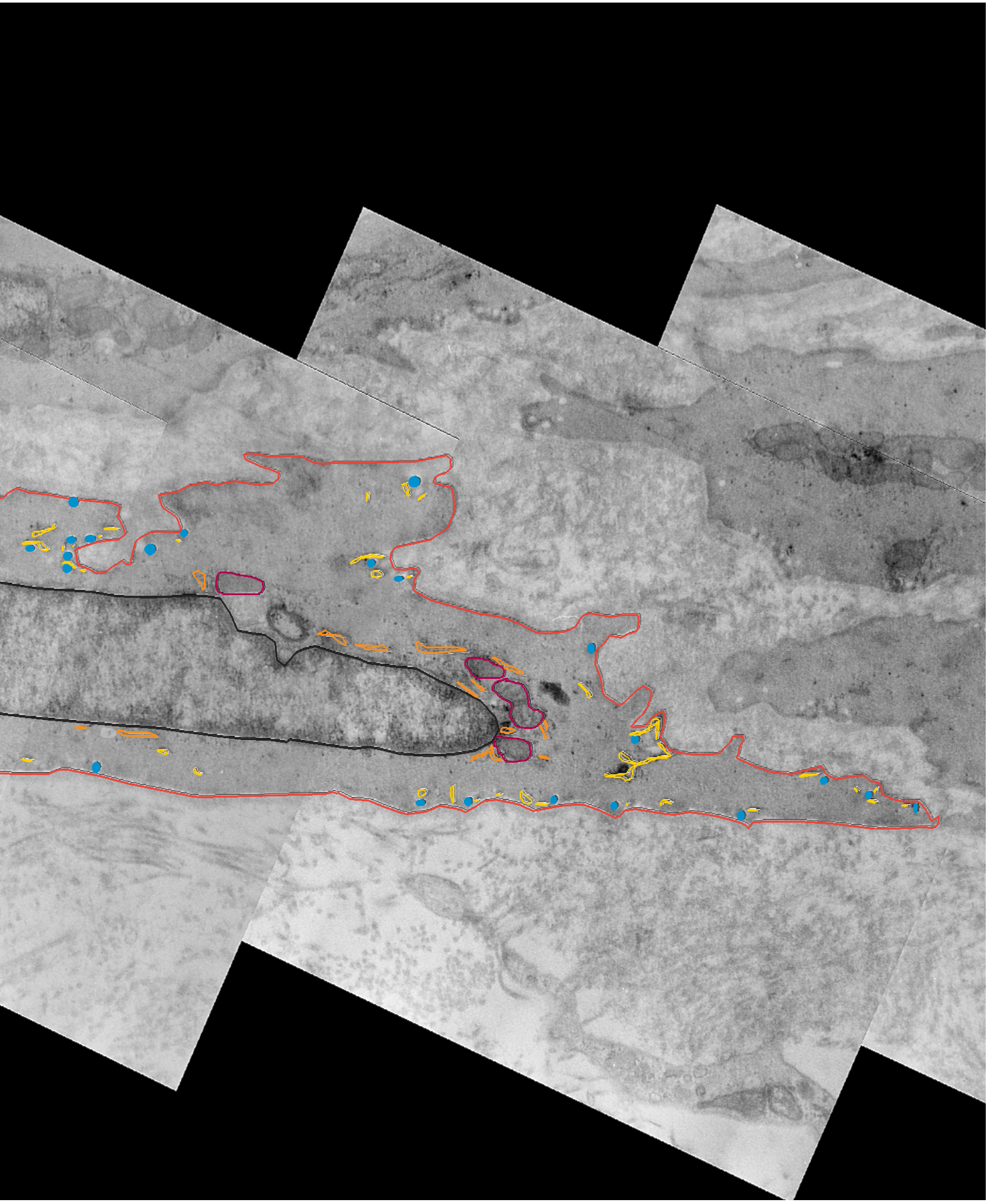

Table 3. Caveolar diameter distribution in visceral and vascular smooth muscle cells.

Caveolar diameter	% of caveolae in visceral SMC (n=100)	% of caveolae in aortic SMC (n=50)
60 - 65 nm	15	16
66 - 70 nm	22	21
71 - 75 nm	24	25
76 - 80 nm	5	22
81 - 85 nm	8	11
86 - 90 nm	8	3
91 - 95 nm	9	2
96 - 100 nm	8	0
>100 nm	1	0

(Table 3). Caveolae showed mainly a round – oval shape (Fig. 10) with a 78 ± 9 nm long diameter (min = 61 nm; max = 108 nm) and a 61 ± 7 nm transverse diameter (min = 60 nm; max = 71 nm). The caveolar diameter in vascular SMCs (Table 3) was about 70 nm (50 caveolae measured: 70.41 ± 8.89 nm; min = 60; max=95).

Fig. 1 (TEM negative images of caveolae) shows, at high magnification, a series of globular or irregular-shaped particles suggesting that these could be protein particles of the so-called caveolar membrane scaffold. Naturally, our images (Fig. 1) do not hint what type of protein(s) they represent (*e.g.* caveolins) and high-resolution immunoelectron microscopy would be required, side by side with molecular biochemistry. Much interest is now focused on caveolae proteomics [44, 51] and more

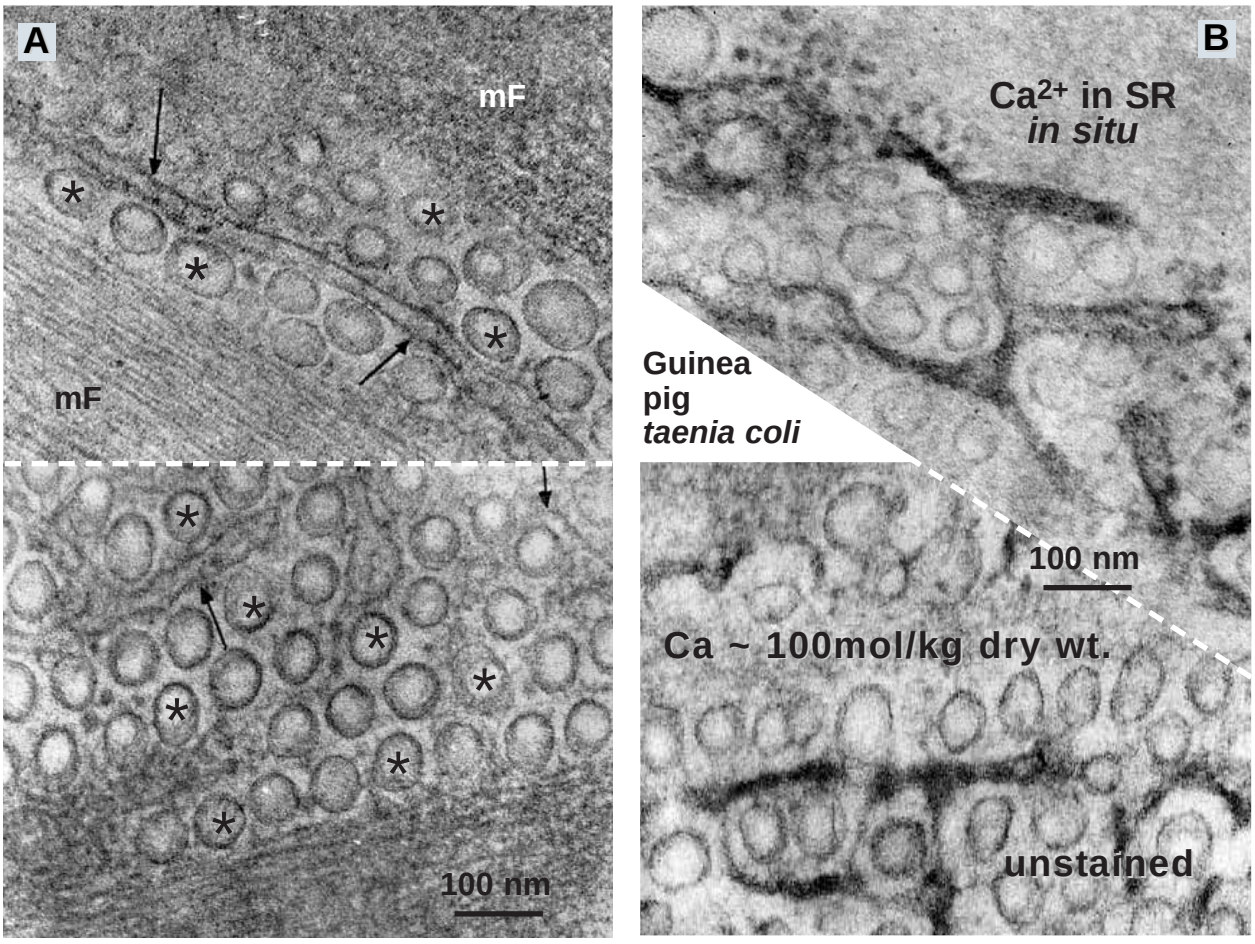

Fig. 7 Tangential ultrathin sections. **A**. Tubules of SR (arrows) can be observed among clusters of cross-sectioned caveolae. **B**. SR tubules showing calcium accumulation (black precipitates inside SR); potassium-oxalate method for *in situ* calcium precipitation, according to the methods of Popescu and Diculescu [28]; Ca concentration in the peripheral SR was estimated by electron-probe microanalysis - signal for Ca at 3.6keV [53].

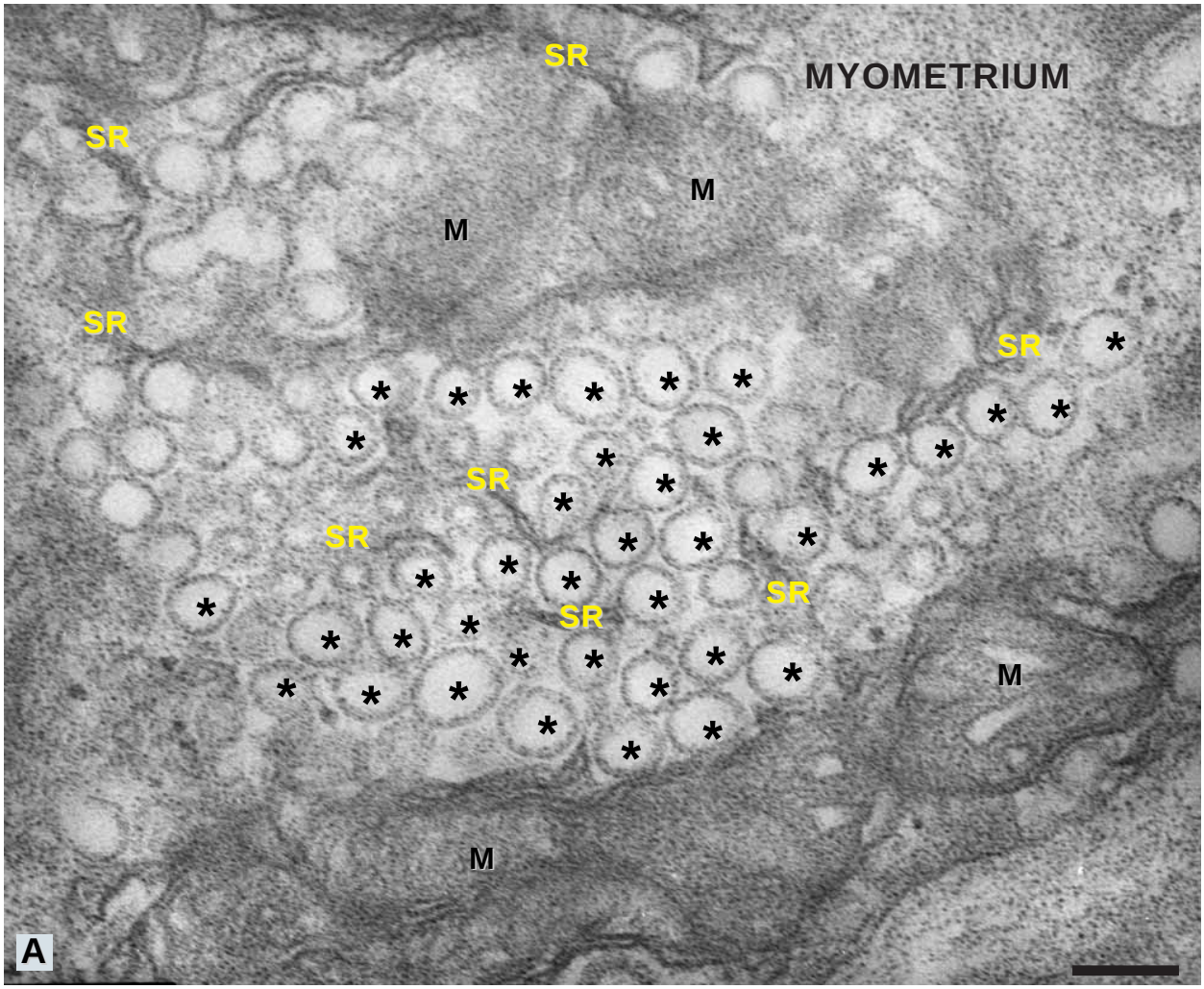

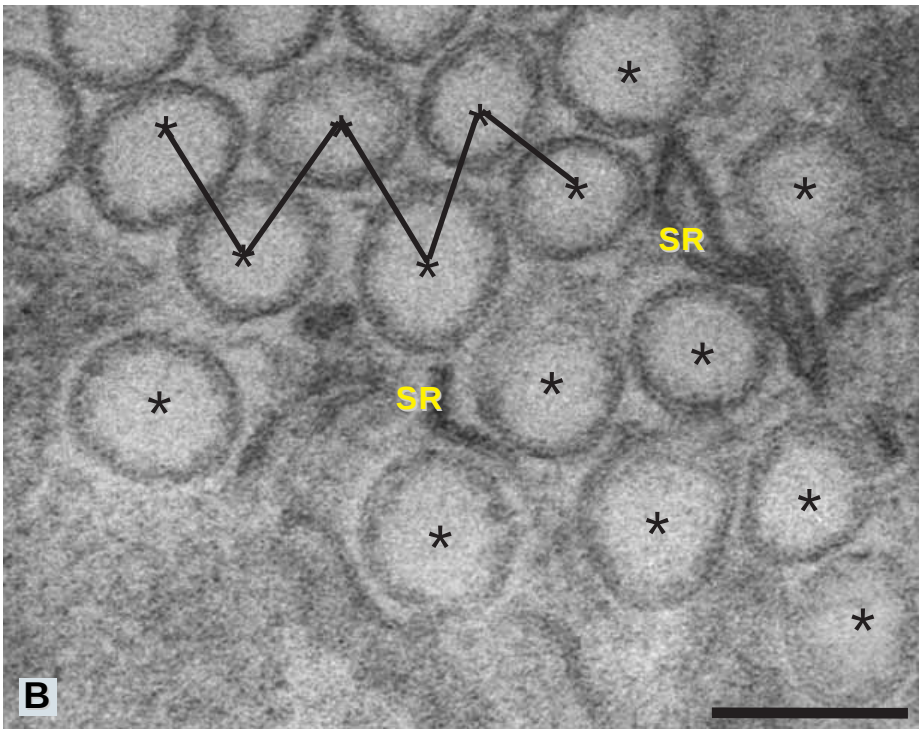

Fig. 8 TEM tangent sections under plasma membrane of SMC from rat *myometrium* (**A**) and *bladder* (**B**). Rows of cross-sectioned caveolae and tubules of SR can be observed. Mitochondria (M) are disposed in the periphery of the caveolar domain. Caveolae seem to have an ordered spatial arrangement in order to acquire the shortest center to center (*) distances. Flask shape of the caveolae main body and *zigzag* caveolar assemblage in the caveolar domains minimize the cytoplasmic volume unavailable for contractile apparatus. Scale bar = 100nm.

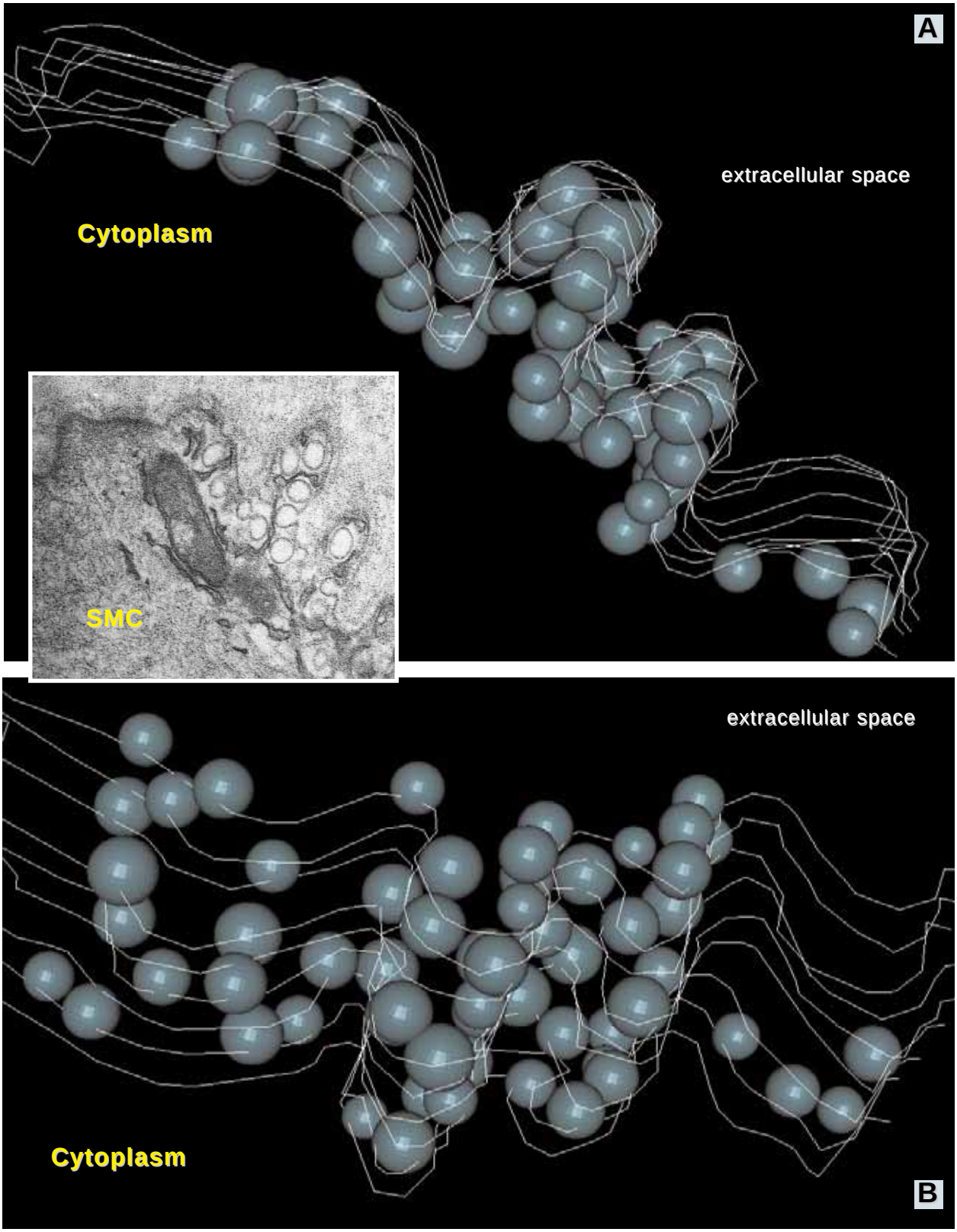

Fig 9. *Rat myometrium* smooth muscle cell. **A, B -** 3D reconstruction from 9 serial TEM sections of the caveolar domain shows the close spatial arrangement of caveolae. Sixty-two caveolae increase plasma membrane area with 59.7%. **B -** lateral view. **Inset -** TEM image of the corresponding portion of the plasma membrane with a wavy appearance. Section no. 3 from 9 serial sections. **Color code**: caveolae - blue spheres; 1μm^2 plasma membrane - white traces.

than 60 types of proteins were found in caveolar membranes [52]. In any case, these electron dense particles, visible in caveolar membrane (Fig. 1) seem more spatiated than in the vicinal non-caveolated plasmalemma.

Usually, individual caveolae open into the extracellular space (Fig. 10A, B) through a constricted neck with a 21 ± 3 nm mean aperture (min = 18 nm; max = 28 nm). A small percent of caveolae 3% (11/330) were clustered around a membrane pocket with a small opening, 20-30 nm wide, toward the extracellular space (Figs. 11–14).

The 3D reconstructed caveolar domains in SMC from rat stomach *muscularis mucosae*, bladder [35] and human ileum (Fig. 12–14) showed plasma membrane finger-like invaginations bearing caveolae that extend into the cytoplasm and generate grape-like clusters. These plasmalemal invaginations are quite irregular in shape (Fig. 14) and could generate the *false image of free intracellular caveolae* near the cellular membrane on single section (Fig. 13). Only one grape-like cluster (1/7) without any contact with SR or mitochondria has been seen (Fig. 12). More than half of these caveolar clusters (4/7) pass through SR sheets and establish close contacts with mitochondria (Fig. 14).

In some very thin TEM sections (less than 30 nm thick; guinea pig *taenia coli*) we found a *diaphragm*, of about 7 nm thick, at the level of caveolar stoma (Fig. 10AB). Anyway, the diaphragm that we observed lacks a central density or knob, as described for endothelial cells [12]. But, Fig. 10C shows that in the case of 'enough lucky' usual TEM sections, a real diaphragm appears as barrier between the proper extracellular space and the interior of caveolae. Finding of SMC caveolar diaphragms in very thin ultrasections, favors the *in situ* existence of caveolar diaphragms, rather than being an artefactual interpretation of TEM images. Naturally, it is more comfortable to disclaim, in some form or another, the presence of diaphragms at the neck (*stoma*) of the smooth muscle caveolae. However, this may simplify too much the presumptive biological reality.

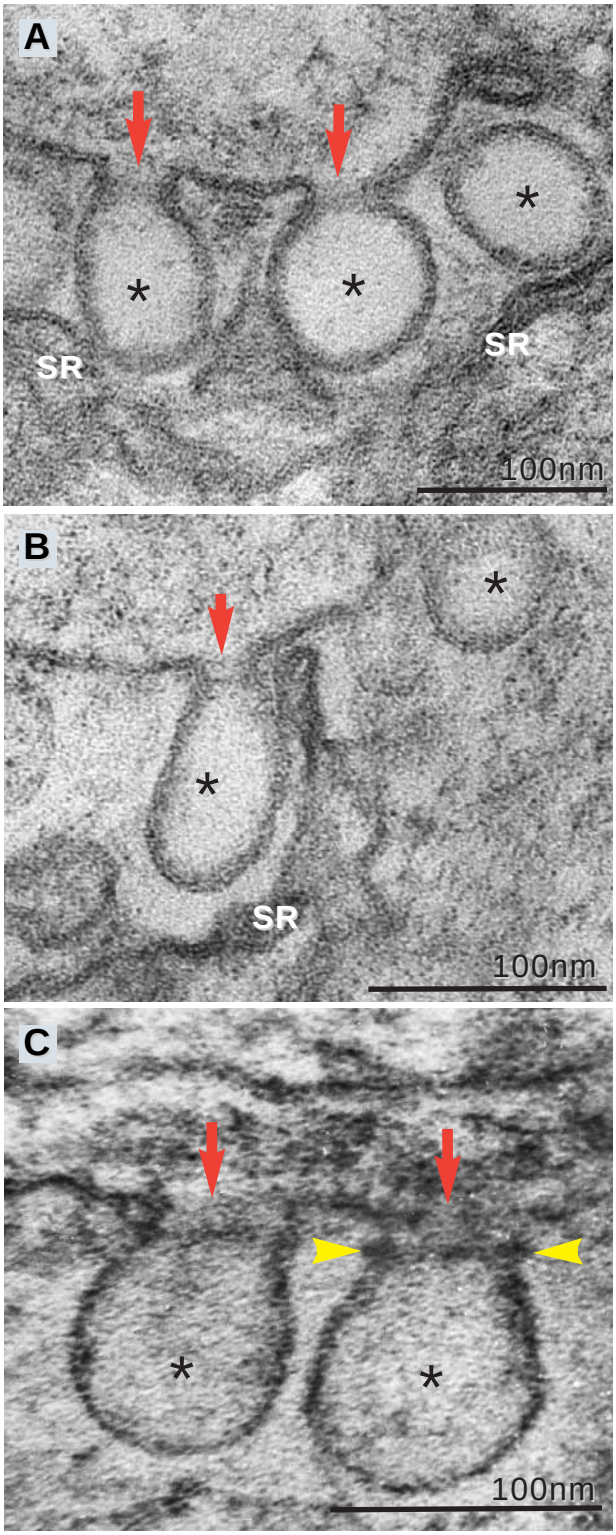

Fig. 10 Guinea pig *taenia coli*. Individual caveolae open into the extracellular space through a neck. A *diaphragm* (arrow) could be seen at the caveolar *stoma* (arrowhead). Caveolae (*) have mainly a round appearance (**A**) but few of them could be oval (**B**). Sarcoplasmic reticulum - SR. **A. B.** - 30 nm ultrathin sections. **C.** - 60 nm thin section; additional prefixation with tannic acid.

Caveolar domain – cortical space of SMC

The reconstitution from adjoining images of a complete longitudinally sectioned SMC showed that the caveolae increase the cellular *perimeter* up to 15%

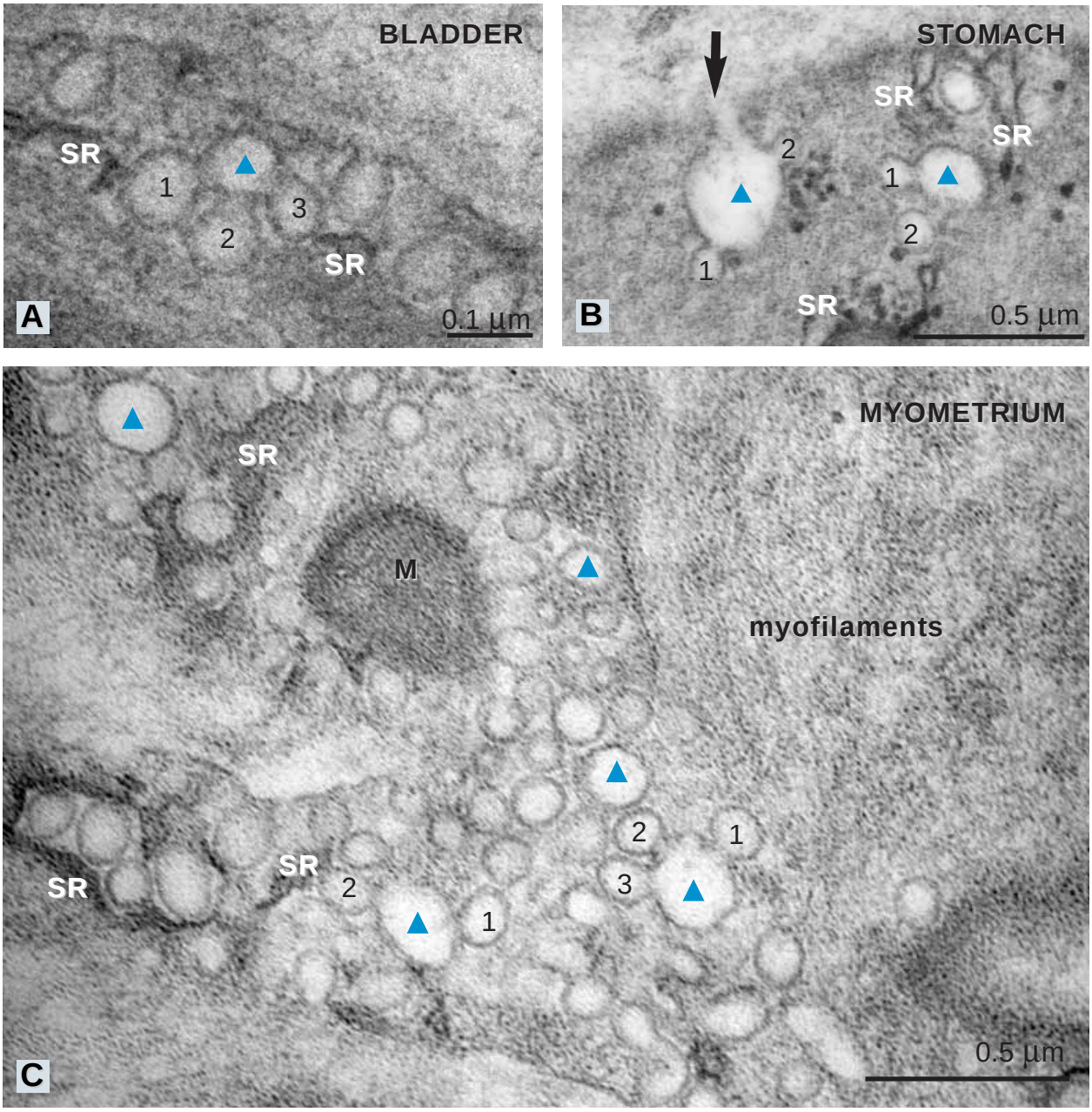

Fig. 11. TEM oblique sections in SMC from rat *bladder* (**A**), *stomach* (**B**), *myometrium* (**C**). Groups of caveolae which do not open directly at the cell surface, but communicate with invaginations of plasma membrane (blue **Δ**). These grape-like clusters show more that 2 caveolae (numbers) which open into the plasma membrane pockets. The invaginations of plasma membrane have a 20-30 small aperture toward extracellular space (arrow). In the area of myofilaments, SR tubules or mitochondria are not visible. Sarcoplasmic reticulum - SR; mitochondria - M.

(Fig. 6). However, the 3D reconstructions of the caveolar domains showed that caveolae enlarge the *surface area* of the plasma membrane over 80% (Fig. 9, 12) and that the peripheral SR and mitochondria are located in the caveolar domains of visceral and vascular SMC (Fig. 3–6, 15–18).

Noteworthy, the 3D reconstructions of 15μ^3 SMC volumes indicated that 87% of caveolae were in close apposition with SR, 10% had close contacts with mitochondria and 3% apparently have no contacts with these organelles. This small fraction of the caveolar population appears in direct vicinity with actin

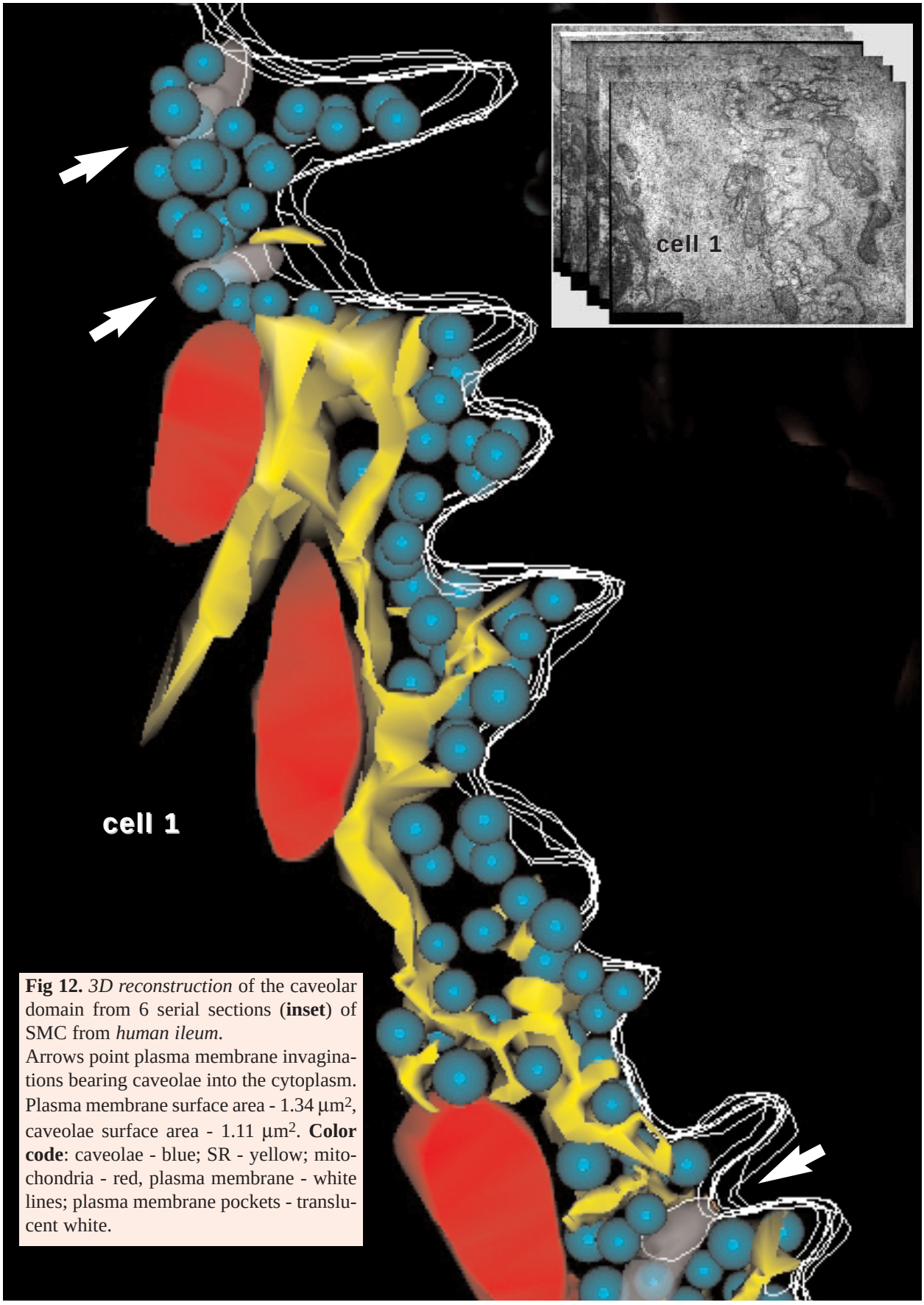

Fig 12. *3D reconstruction* of the caveolar domain from 6 serial sections (**inset**) of SMC from *human ileum.*
Arrows point plasma membrane invaginations bearing caveolae into the cytoplasm. Plasma membrane surface area - 1.34 μm^2, caveolae surface area - 1.11 μm^2. **Color code**: caveolae - blue; SR - yellow; mitochondria - red, plasma membrane - white lines; plasma membrane pockets - translucent white.

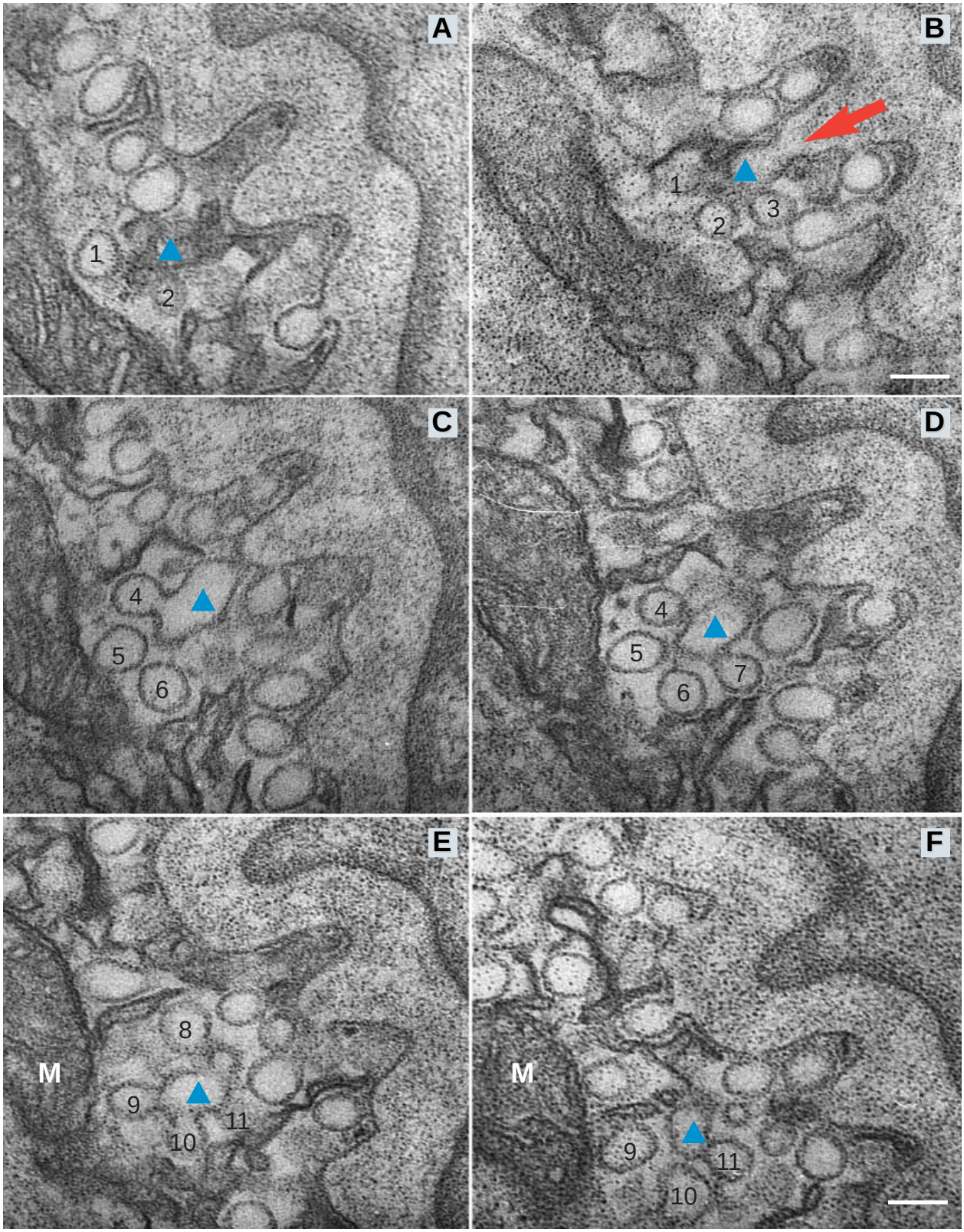

Fig. 13 A–F. Serial sections (less than 35 nm thick) through a grape-like structure with 11 caveolae (numbers). A 22 nm wide opening (arrow) of the membrane pocket (blue Δ) could be seen only in one section (**B**). Plasmalemmal invagination brings caveolae toward mitochondria (M). SMC from *human ileum*. Scale bar = 100nm.

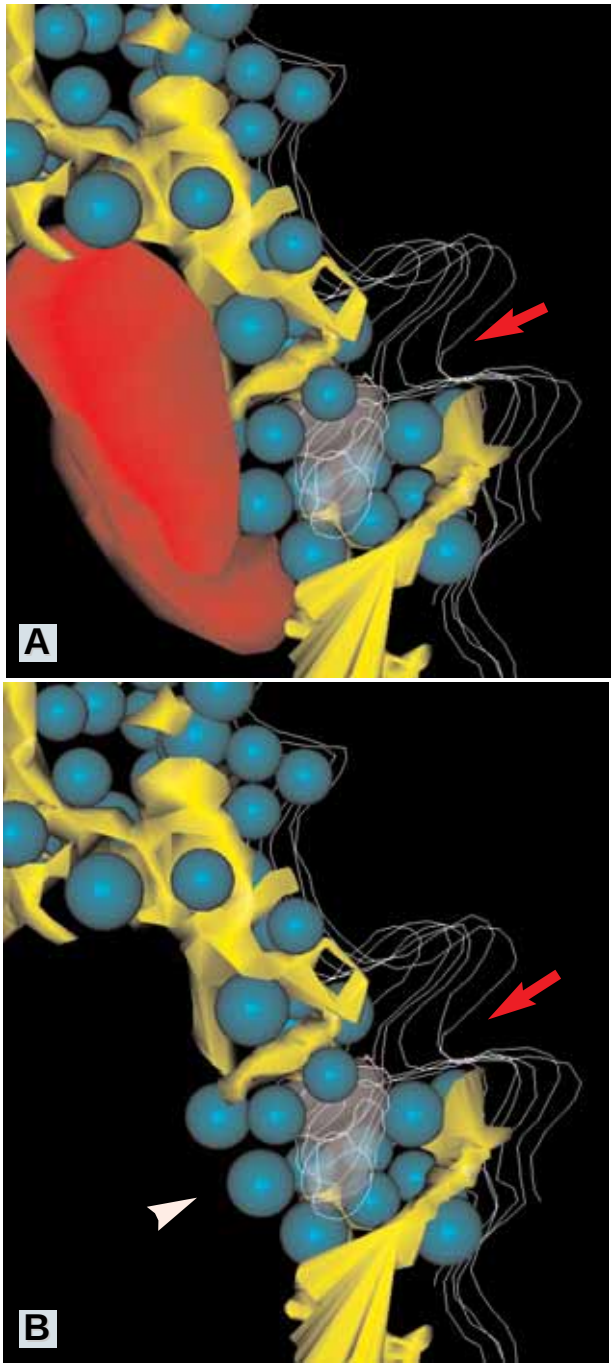

Fig. 14 A. 3D reconstructed volume of the grape-like caveolar cluster from TEM sections in *Fig. 10*. Plasmalemmal invagination (arrow) has an irregular shape and carries caveolae deeply into the cytoplasm towards mitochondria. **B.** Exclusion of the mitochondria from the reconstructed volume shows that this membranar pocket splits apart the SR sheets (arrowhead) in order to have a direct contact with the mitochondria. **Color code:** caveolae - blue; SR - yellow; mitochondria - red, plasma membrane - white lines; plasma membrane pockets - translucent white. SMC from *human ileum.*

bundles (Fig. 15, 16). Remarkably, it was recently demonstrated by electron tomography that spatially restricted signals could redistribute receptors to a limited subset of caveolae, and in addition actin filaments could recruit nearby caveolae at specific sites to influence signaling [54].

In the 3D reconstructed volumes from serial sections, the caveolae without close contacts with SR or mitochondria were very few (Fig. 12) but a single section, apparently, *isolated* caveolae could be seen (Fig. 15, 16), leading to the erroneous conclusion that they are numerous. *We are inclined to believe that isolated caveolae, without apposition of peripheral SR and mitochondria, are an exception rather than a rule.*

Organelles nanocontacts

Our images show that caveolae establish contacts (nanocontacts), directly or mediated by molecular complexes (nanostructures), with SR (Fig. 5, 7, 8, 12, 15–22), mitochondria (Fig. 13, 14, 18, 22, 23), myofilaments (Fig. 15, 16) and perinuclear cisterna of the nuclear envelope (Fig. 24) in the visceral and vascular SMC.

Usually, about 15 nm wide electron-transparent *junctional spaces* (Table 4) exist between caveolae and SR [35]. We have also identified nanostructural links between caveolae and SR, mitochondria or perinuclear cisterna, which is supposed to communicate with SR (Table 4). Two types of *nanostructural links* have been identified between caveolae and SR or mitochondria: *direct contacts* between membranes (gap/space < 2 nm or *none*) (Fig. 19, 20) and *electron-dense structures* between membranes about 12 nm wide (Fig. 19–22).

A special relationship (nanocontacts) was observed between caveolae and the perinuclear cisterna, a particular domain of the smooth endoplasmic reticulum (mainly sarcoplasmic reticulum) (Fig. 24A,C). Of course, such nanocontacts appear in the *lateral* perinuclear space. Our previous works [27, 29] have clearly shown that perinuclear cisterna is a calcium storage site. Fig. 25A,B provides new additional support. Thus, a possible paradigm of excitation-transcription coupling in smooth muscle arises [55].

Table 4. Caveolar nanocontacts in visceral and vascular smooth muscle cells.

	Caveolae-SR (n= 50)	**Caveolae-mitochondria** (n= 25)	**Caveolae-perinuclear cisterna** (n= 10)
mean distance between organelles	15.47 ± 4.91 nm	15.69 ± 7.39 nm	14.97 ± 3.5 nm
mean dimension of feet-like structures	11.84 ± 2.41 nm	12.32 ± 4.56 nm	10.27 ± 2 nm

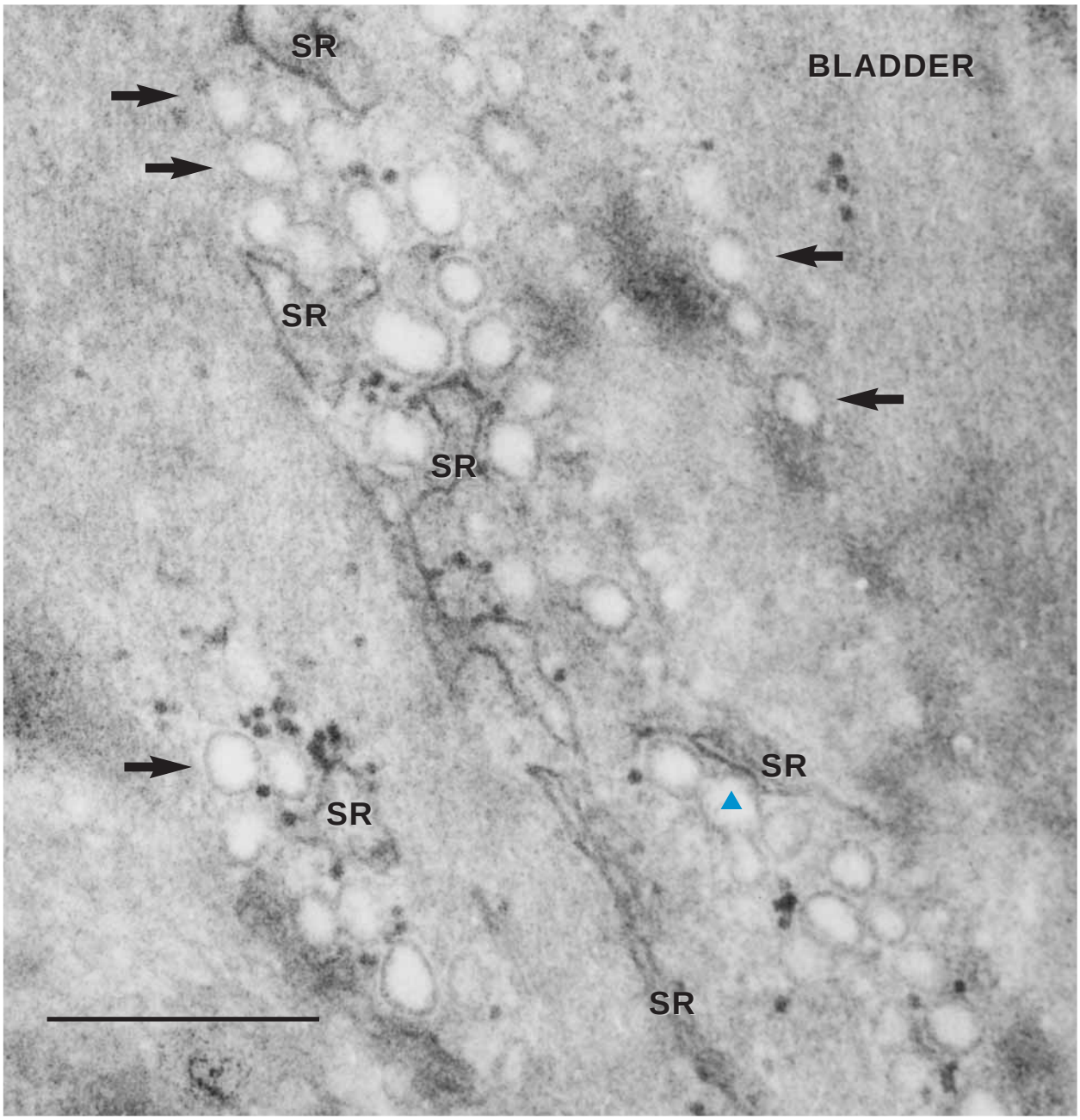

Fig. 15 SMC sectioned beneath plasma membrane. Most of caveolae are cross-sectioned and a labyrinthic system of sarcoplasmic reticulum (SR) is spread around them. Few caveolae directly face the cytoplasm having contacts with myofilaments (arrows). Grape-like caveolar structure - blue Δ. Bladder. Scale bar = 0.5 μm.

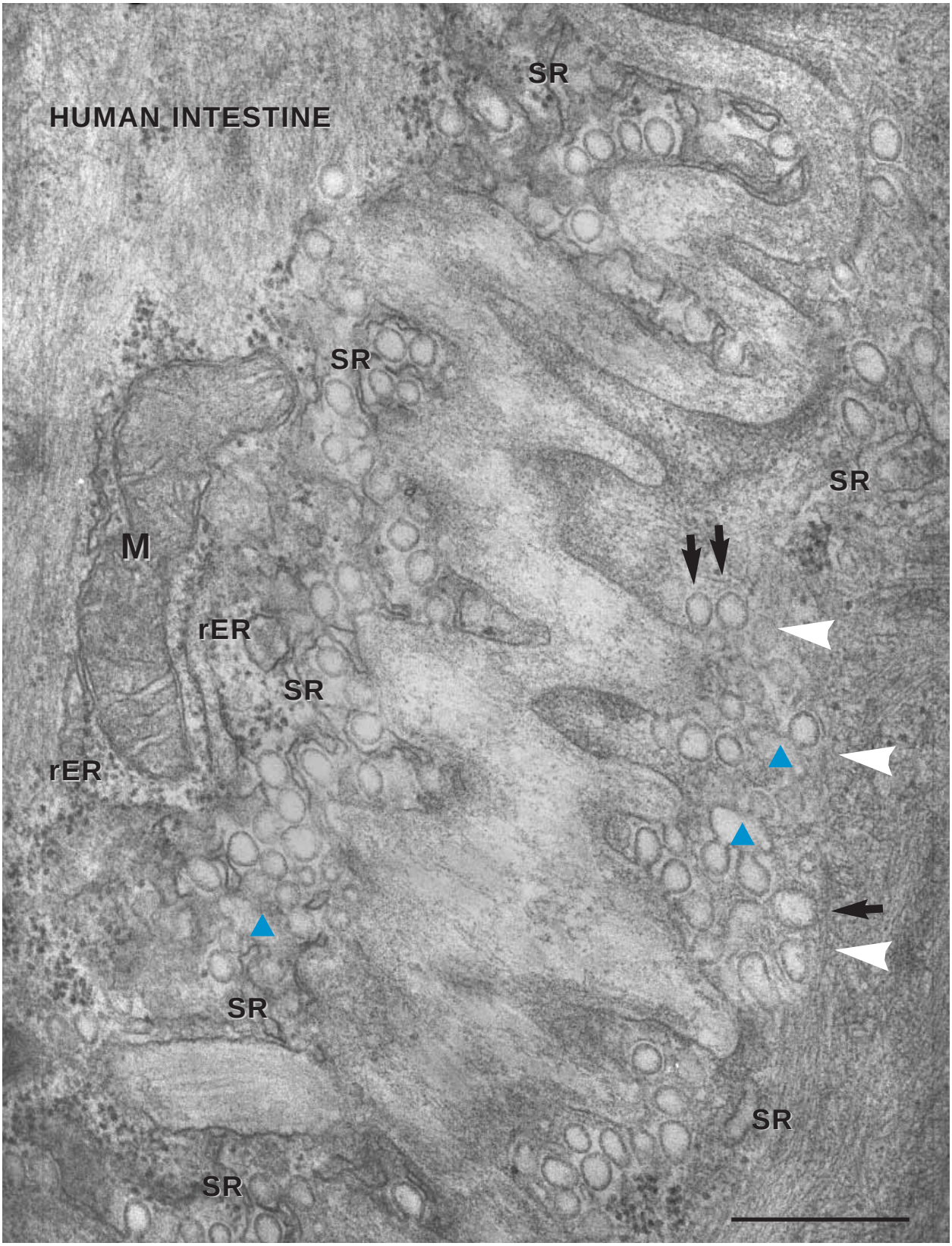

Fig. 16 Contracted SMC have irregular folds on its surface giving a wavy appearance. Rough ER (rER) could be seen in the caveolar domain. Grape-like caveolar clusters (blue Δ). Some myofilaments seem very near to caveolae (arrows) in caveolar domains without visible interpolation of SR (arrowhead). SMC from human ileum. Scale bar = 0.5 μm.

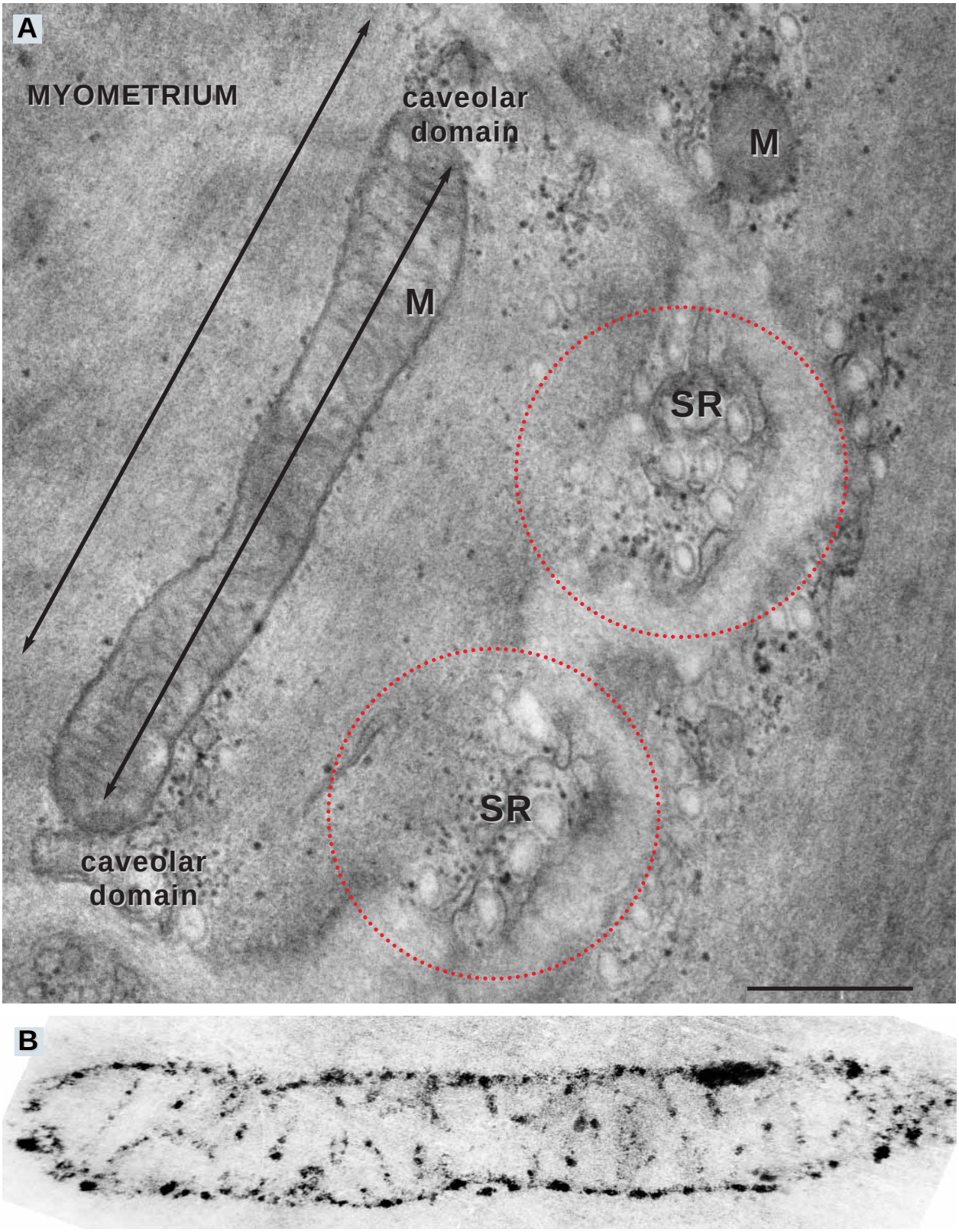

Fig. 17 **A.** An oblique section through rat *myometrum* SMC showing one long mitochondrion (M) parallel with myofilaments and establishing contacts with two areas of the caveolar domain. SR tubules surround caveolae (round mark). Scale bar = 0.5 µm. **B.** A comparable mitochondrion showing calcium oxalate precipitates (black dots) after *in situ* calcium precipitation, according to the potassium-oxalate method described in [27].

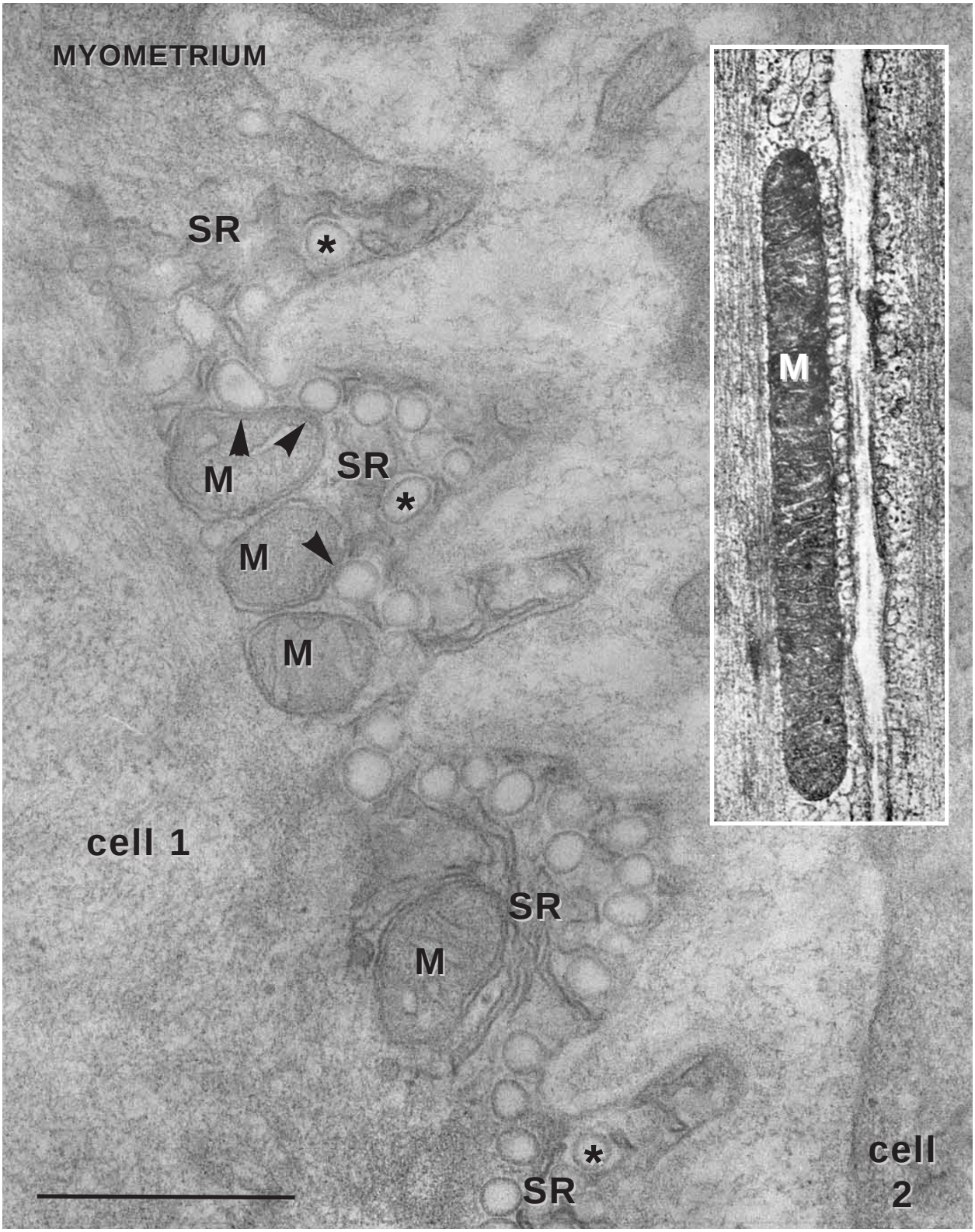

Fig. 18 Caveolar domain (cell 1) opposite to non-caveolar domain (cell 2) in SMC from *myometrium*. Almost all caveolae have close contacts with SR. Junctional spaces could be seen between caveolae and SR (*). Few caveolae have a direct contact (arrowhead) with mitochondria (M). Sometimes mitochondria could have close apposition with more than 10 caveolae. Scale bar = 0.5 μm. **Inset -** SMC from guinea pig *taenia coli*, fixed under ismoetric conditions; nanocontacts of a long peripheral mitochondrion with at least 25 caveolae).

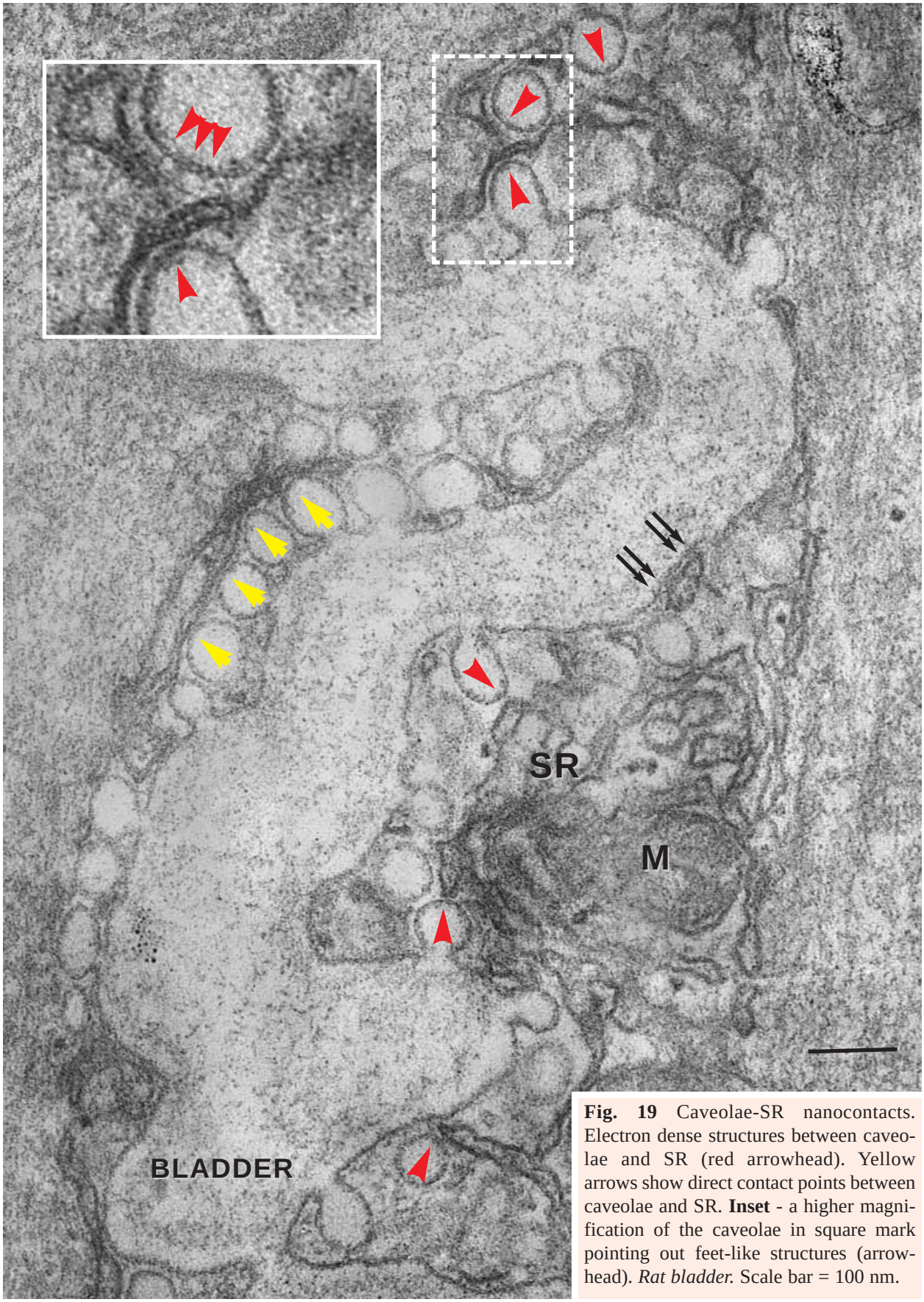

Fig. 19 Caveolae-SR nanocontacts. Electron dense structures between caveolae and SR (red arrowhead). Yellow arrows show direct contact points between caveolae and SR. **Inset** - a higher magnification of the caveolae in square mark pointing out feet-like structures (arrowhead). *Rat bladder.* Scale bar = 100 nm.

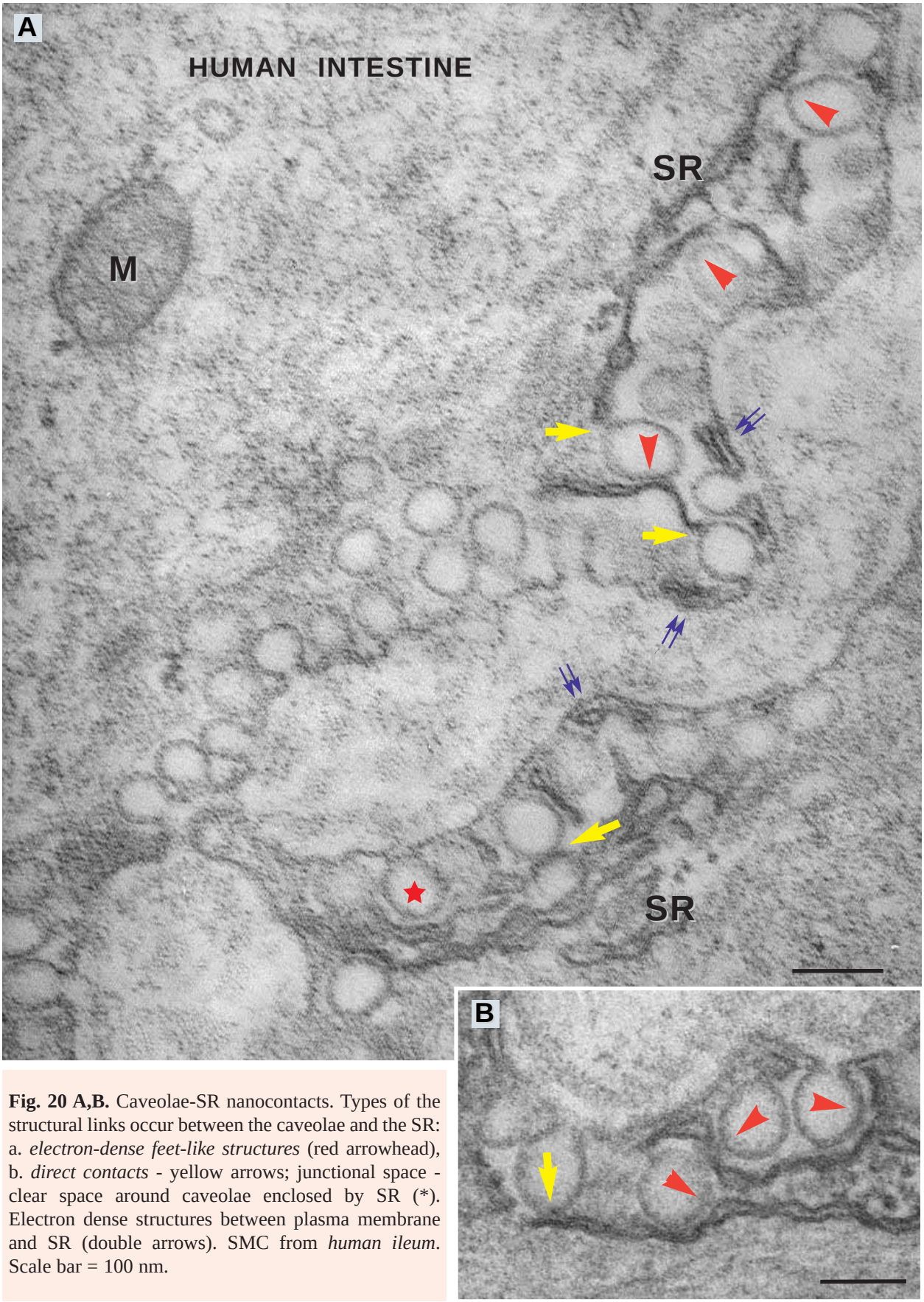

Fig. 20 A,B. Caveolae-SR nanocontacts. Types of the structural links occur between the caveolae and the SR: a. *electron-dense feet-like structures* (red arrowhead), b. *direct contacts* - yellow arrows; junctional space - clear space around caveolae enclosed by SR (*). Electron dense structures between plasma membrane and SR (double arrows). SMC from *human ileum*. Scale bar = 100 nm.

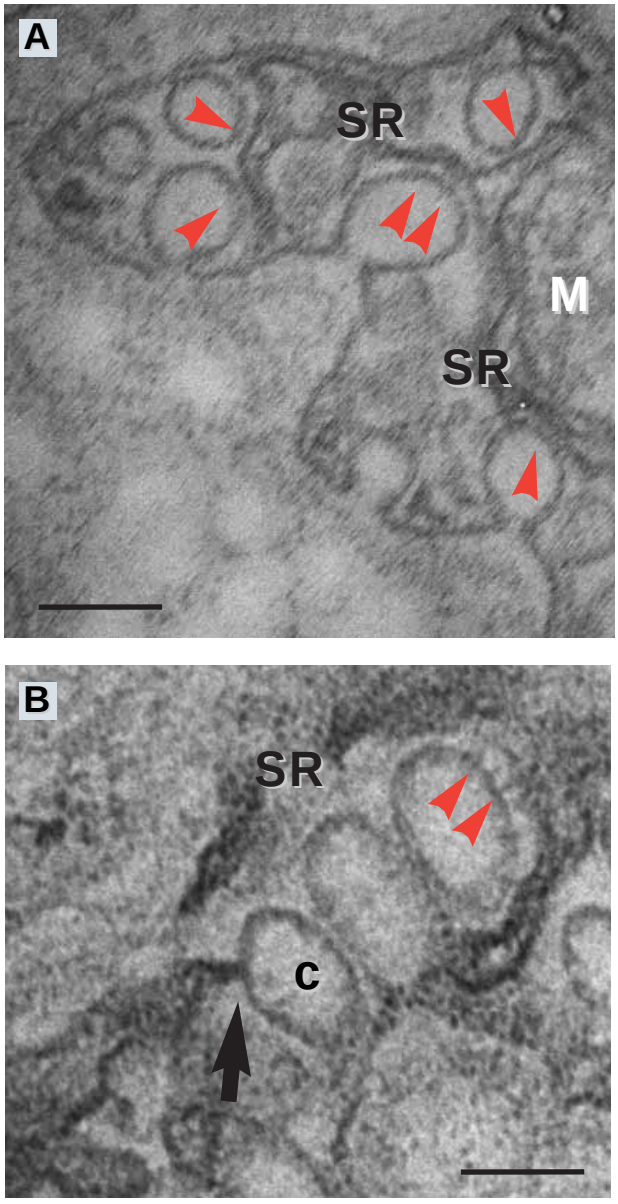

Fig. 21 A,B. Caveolae-SR nanocontacts. Electron dense structures (arrowhead) and direct contact (arrow) between caveolae and SR. SMC from human ileum. Scale bar = 50 nm.

The mean distance between caveolae and perinuclear cisterna was about 15 nm, but 10 nm 'feet'-like nanostructures were also observed (Fig. 24C inset). In addition, the plasma membrane invaginations bearing caveolae have been seen in the neighborhood of the nucleus (Fig. 24B).

Concluding remarks

Our results sustain the existence of complex connections of caveolae with peripheral sarcoplasmic reticulum, mitochondria and perinuclear cisterna of the nuclear envelope. This study presents unequivocal ultrastructural evidence for direct physical (morphological) interactions of SMC caveolae with peripheral (subplasmalemmal) organelles. Our conclusions are based on high resolution electron microscopy, *ultrathin serial sections* and *computer aided 3D reconstructions*.

a. **The main interaction occurs between caveolae and peripheral SR.** Our previous ultracytochemical works [21, 27–29, 53, 56] (see also Fig. 7, p. 971, this study) revealed SR, particularly peripheral SR as the main Ca accumulating and releasing intracellular organelle, implicated in contraction-relaxation cycle. Anyway the current literature is abundant in this respect (*e.g.* [57–63]).

We were particularly encouraged to believe that the range of Ca concentration measured by electron probe X-ray microanalysis in SMC-SR *in situ* (on thin unstained sections), ~100 mmol/kg dry wt. [53], is not an instrumental artifact, because independent atomic absorption measurements of the endogenous Ca content in isolated microsomal fraction (representative for SR, and maybe for caveolae) indicated 122±26 mmol Ca/kg dry wt. Moreover, the reported Ca concentrations measured by X-ray microanalysis in the terminal cisternae of SR from skeletal muscle were (mmol/kg dry wt.): 97±21 [53] or 117±48 [57].

We describe here two types of nanocontacts caveolae-peripheral SR:

1. *Direct contact, without feet-like structures*, the free space between the two membranes being less than 2nm (Fig. 19, 20);
2. *Mediated contact, with linking feet-like structures* (Fig. 19–21). We can not establish at this moment whether such linking nanostructures ('nano-rods') involve or not RyR, as those described by others [38, 39].

Anyway, it has to be mentioned that we confirm contacts of peripheral SR (junctional SR), which are established with a cytoplasmic side of plasmalemma (Fig. 19, 20). Such contacts were long time ago supposed to exist [37] and unequivocally shown by ultrathin serial sections [35] and this study.

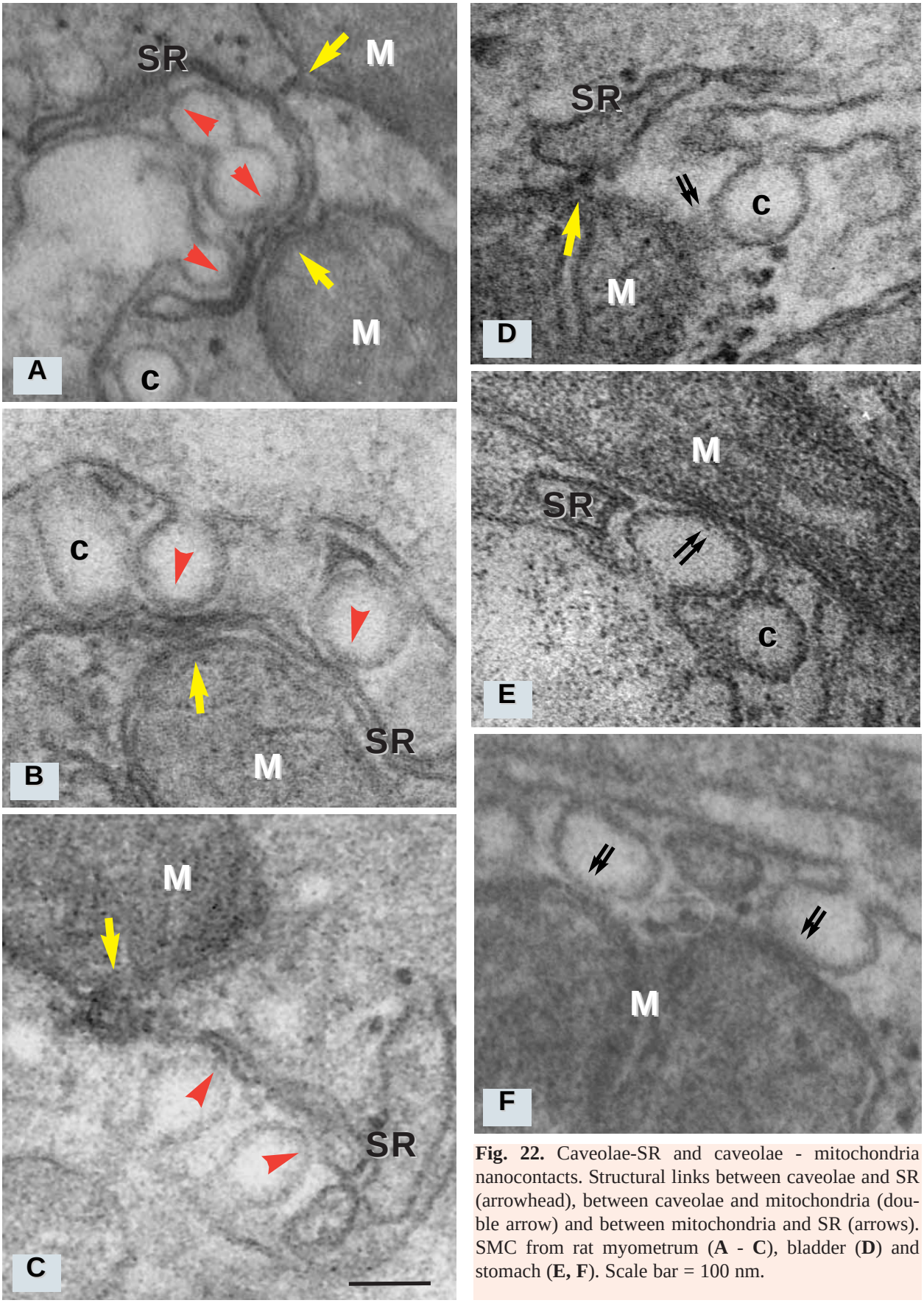

Fig. 22. Caveolae-SR and caveolae - mitochondria nanocontacts. Structural links between caveolae and SR (arrowhead), between caveolae and mitochondria (double arrow) and between mitochondria and SR (arrows). SMC from rat myometrum (**A** - **C**), bladder (**D**) and stomach (**E, F**). Scale bar = 100 nm.

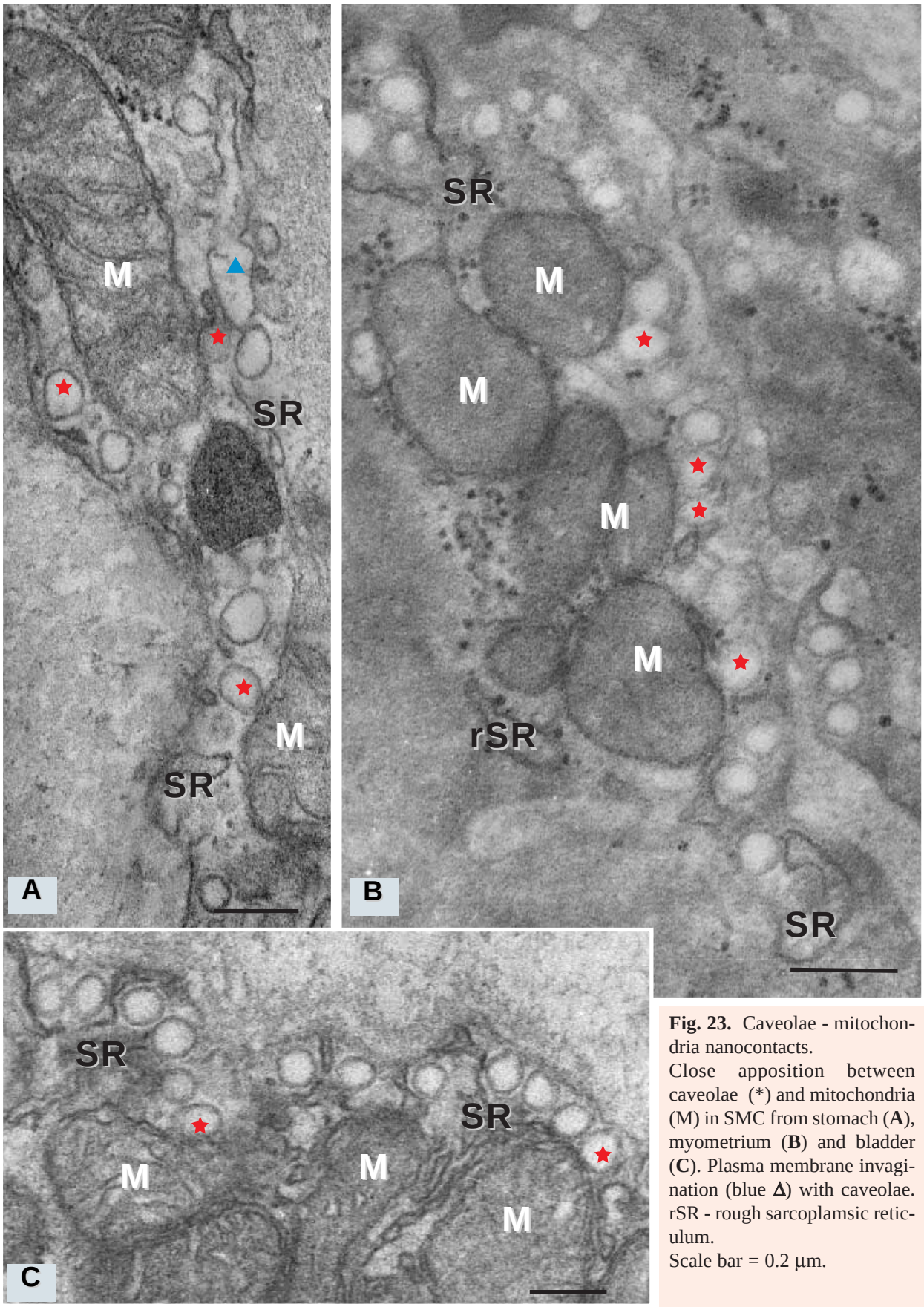

Fig. 23. Caveolae - mitochondria nanocontacts.
Close apposition between caveolae (*) and mitochondria (M) in SMC from stomach (**A**), myometrium (**B**) and bladder (**C**). Plasma membrane invagination (blue **Δ**) with caveolae. rSR - rough sarcoplamsic reticulum.
Scale bar = 0.2 μm.

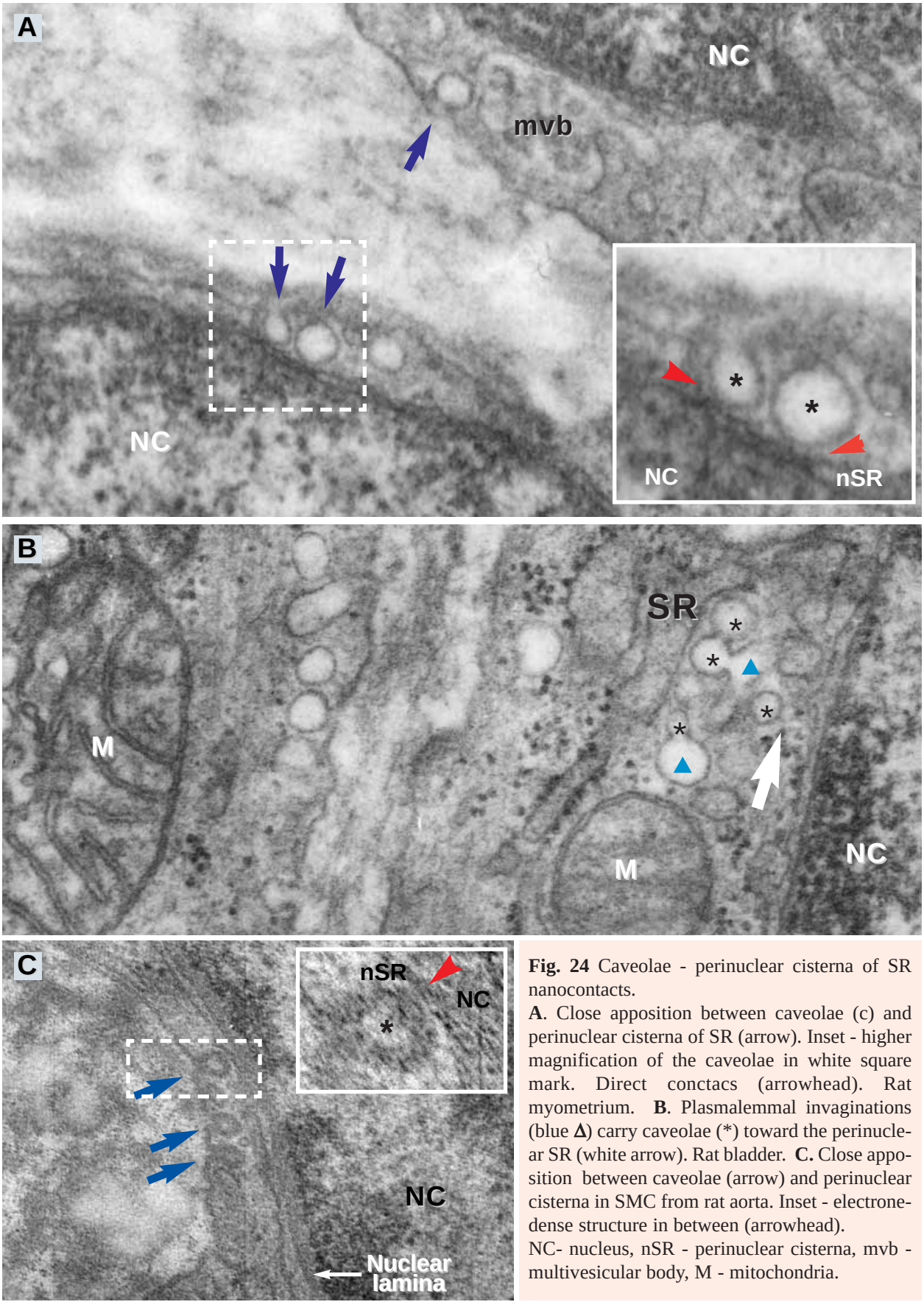

Fig. 24 Caveolae - perinuclear cisterna of SR nanocontacts.
A. Close apposition between caveolae (c) and perinuclear cisterna of SR (arrow). Inset - higher magnification of the caveolae in white square mark. Direct conctacs (arrowhead). Rat myometrium. **B**. Plasmalemmal invaginations (blue Δ) carry caveolae (*) toward the perinuclear SR (white arrow). Rat bladder. **C.** Close apposition between caveolae (arrow) and perinuclear cisterna in SMC from rat aorta. Inset - electrone-dense structure in between (arrowhead).
NC- nucleus, nSR - perinuclear cisterna, mvb - multivesicular body, M - mitochondria.

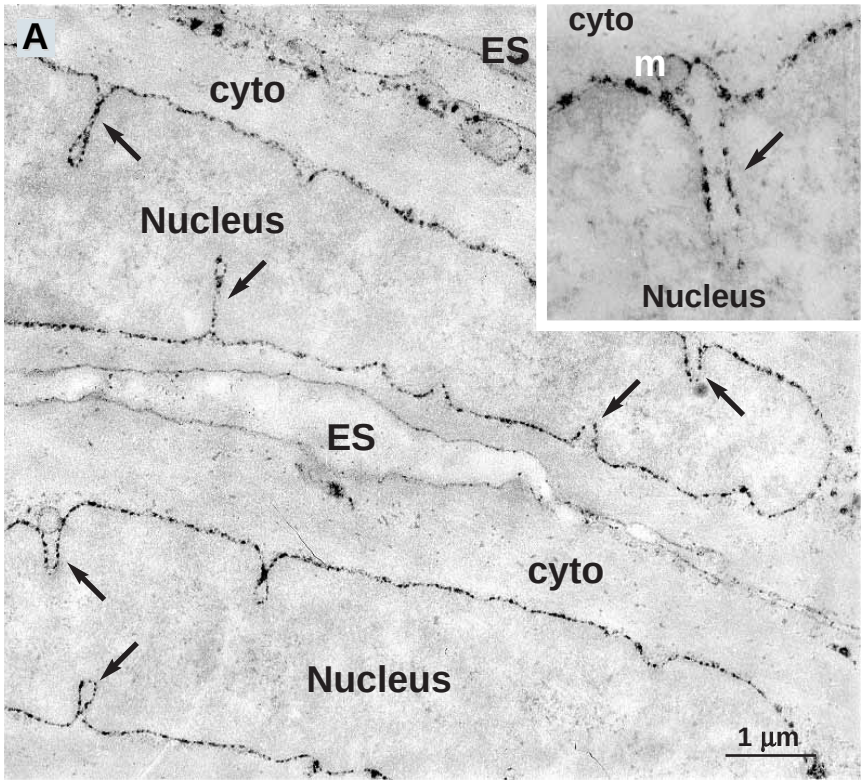

Fig. 25 A. **Calcium localization in SMC** under isotonic contraction; note the indentations of the nuclear envelope, which are characteristic for this situation, corresponding to the classical 'corkscrew' described by light microscopists. Abundant black precipitates of calcium oxalate fill the space of the perinuclear cisterna which surrounds the nucleus. **Inset**: a mitochondrion in contact with the perinuclear cisterna and an element of SR, emerging from the nuclear envelope. Potassium-oxalate method, according to Popescu *et al.* [27]. Pig coronary artery. *Unstained*. ES, extracellular space. **B**. SMC of *taenia coli*, fixed under relaxation. Calcium oxalate precipitates mark clearly the perinuclear cisterna. Ultracytochemical method described in ref. [28]. Lead citrate staining *only*.

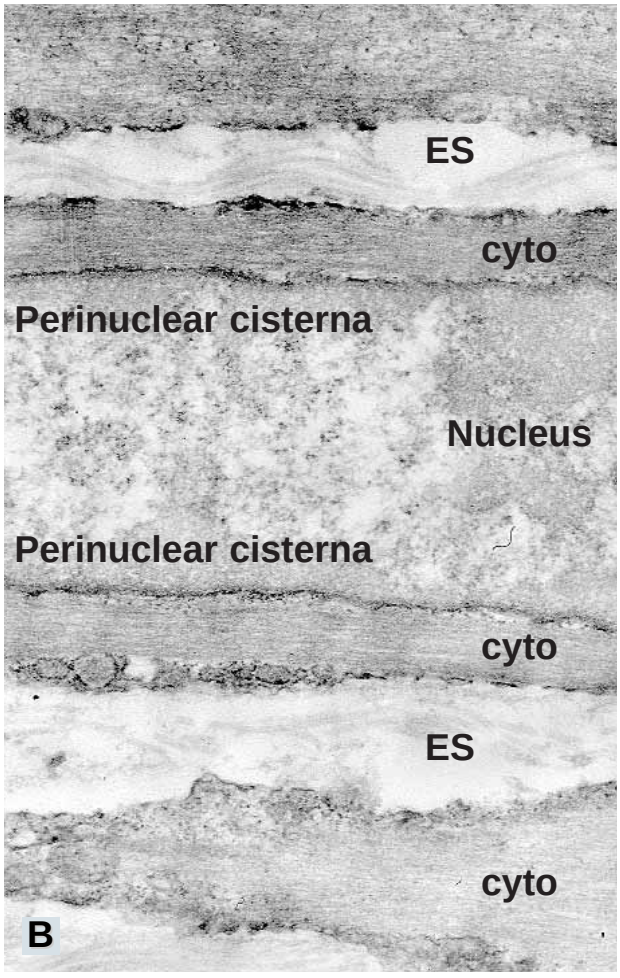

Last but not least, as concerns the caveolae-SR interactions, we would like to emphasize that the frequency of the so-called 'Ca^{2+} release units' [38] in smooth muscle is much higher than once believed. For instance, in one of our recent articles [35], at least 17 (!) such calcium release units can be counted, in only one image (Fig. 1B, p. 521 [35]).

b. **Interaction of caveolae with mitochondria.** Two types of nanocontacts were found at high magnification in SMC:

1. *Direct contact*, without the interposition of feet-like structures (Fig. 18), or
2. *Mediated contact*, *via* feet-like structures (Fig. 22).

Although the possible role of mitochondria in the regulation of contraction-relaxation cycle, particularly in the excitation-contraction coupling, was denied about 20 years ago, nowadays the role of mitochondria in the intracellular Ca^{2+} homeostasis is again considered (*e.g.* [26, 64–66]). Moreover, we found in SMC relatively frequent contacts between mitochondria and SR (Fig. 18, 19, 22, 23), and some sort of threads as linkage between endoplasmic reticulum and mitochondria was described [67].

For the moment, the molecular exchanges between SR and mitochondria *in situ* remain in the field of speculations. As concerns the nanocontacts caveolae-mitochondria, some possible candidates for molecular translocations (besides ions) seems to be cholesterol or other lipids (see [24, 25]).

A simple additional explanation of nanocontacts might be to keep the organelles in close proximity in a very dynamic interior of SMC.

c. **Nanocontacts between caveolae and perinuclear cisterna** suggest the possible implication of nuclear envelope in signaling, directly from outside the cell, bypassing the cytoplasm (Fig. 24, 25). In this way, caveolae could be implicated in **excitation-transcription coupling** [55].

d. Our results, particularly the 3D reconstructions from serial ultrathin sections (Fig. 12–14) highlight the idea that caveolae, SR and mitochondria form **an unique, peripheral (cortical) continuum compartment** in SMC. In fact, this subplasmalemmal compartment could be regarded as **a 'super-Ca^{2+} release/storage unit'**.

Finally, we propose, extrapolating concepts from developmental embryology [68], that **SMC caveolae** might be **'carriers' of positional information**.

Acknowledgments

Part of this study was supported by a grant VIASAN (391/2004) from the Ministry of Education and Science.

We thank Prof. Clara Franzini-Armstrong for valuable questions and suggestions concerning 'feet'-like electron-dense structures.

References

1. **Palade GE.** Fine structure of blood capillaries. *J Appl Physiol*. 1953; 24: 1424–36
2. **Yamada E.** The fine structure of the gall bladder epithelium of the mouse. *J Biophys Biochem Cytol*. 1955; 1: 445-458
3. **Anderson RGW.** The caveolae membrane system. *Annu Rev Biochem*. 1998; 67: 199-225
4. **Ostrom RS, Insel PA**. Caveolar microdomains of the sarcolemma: compartmentation of signaling molecules comes of age. *Circ Res*. 1999; 84: 1110-2
5. **Fujimoto T.** Cell biology of caveolae and its implication for clinical medicine. *Nagoya J Med Sci*. 2000; 63: 9-18
6. **Taggart MJ**. Smooth muscle excitation-contraction coupling: a role for caveolae and caveolins? *News Physiol Sci*. 2001; 16: 61-5
7. **Stan RV**. Structure and function of endothelial caveolae. *Microsc Res Tech*. 2002; 57: 350-64
8. **Parton RG.** Caveolae - from ultrastructure to molecular mechanisms. *Nat Rev Mol Cell Biol*. 2003; 4: 162–7
9. **Cohen AW, Hnasko R, Schubert W, Lisanti MP**. Role of caveolae and caveolins in health and disease. *Physiol Rev*. 2004; 84: 1341-79
10. **Bergdahl A, Sward K**. Caveolae-associated signalling in smooth muscle. *Can J Physiol Pharmacol*. 2004; 82: 289-99
11. **White MA, Anderson RGW**. Signaling networks in living cells. *Annu Rev Pharmacol Toxicol*. 2005; 45: 587-603
12. **Stan RV.** Structure of caveolae. *Biochim Biophys Acta*. 2005; 1746: 334-48
13. **Daniel EE, El-Yazbi A, Cho WJ.** Caveolae and calcium handling, a review and a hypothesis. *J Cell Mol Med*. 2006; 10: 529-44
14. **Bolton TB**. Calcium events in smooth muscles and their interstitial cells; physiological roles of sparks. *J Physiol*. 2006; 570: 5-11
15. **van Meer G**. The different hues of lipid rafts. *Science*. 2002; 296: 855-7
16. **van Deurs B, Roepstorff K, Hommelgaard AM, Sandvig K**. Caveolae: anchored, multifunctional platforms in the lipid ocean. *Trends Cell Biol*. 2003; 13: 92-100
17. **Munro S**. Lipid rafts: elusive or illusive? *Cell*. 2003; 115: 377-388
18. **Hardin CD, Vallejo J**. Caveolins in vascular smooth muscle: form organizing function. *Cardiovasc Res*. 2006; 69: 808-15
19. **Anderson RGW**. Potocytosis of small molecules and ions by caveolae. *Trends Cell Biol*. 1993; 3: 69-72
20. **Pelkmans L, Kartenbeck J, Helenius A**. Caveolar endocytosis of simian virus 40 reveals a new two-step vesicular-transport pathway to the ER. *Nature Cell Biol*. 2001; 3: 473-83
21. **Popescu LM**. Conceptual model of the excitation-contraction coupling in smooth muscle; the possible role of the surface microvesicles. *Studia Biophysica (Berlin)*. 1974; 44: 141-53
22. **Ingber DE.** Cellular mechanotransduction: putting all the pieces together again. *FASEB J*. 2006; 20: 811-27
23. **Yu J, Bergaya S, Murata T, Alp IF, Bauer MP, Lin MI, Drab M, Kurzchalia TV, Stan RV, Sessa WC.** Direct evidence for the role of caveolin-1 and caveolae in mechanotransduction and remodeling of blood vessels. *J Clin Invest*. 2006; 116: 1222-5
24. **Fielding CJ, Fielding PE.** Relationship between cholesterol trafficking and signaling in rafts and caveolae. *Biochim Biophys Acta*. 2003; 1610: 219-28
25. **Martin S. Parton RG.** Caveolin, cholesterol, and lipid bodies. *Sem Cell Dev Biol*. 2005; 16: 163-74

26. **Rizzuto R, Pozzan T**. Microdomains of intracellular Ca2+: molecular determinants and functional consequences. *Physiol Rev*. 2006; 86: 369–408
27. **Popescu LM, Diculescu I, Zelck U, Ionescu N**. Ultrastructural distribution of calcium in smooth-muscle cells of guinea-pig taenia coli - correlated electron-microscopic and quantitative study. *Cell Tiss Res*. 1974; 154: 357–78
28. **Popescu LM, Diculescu I**. Calcium in smooth muscle sarcoplasmic reticulum in situ. Conventional and X-ray analytical electron microscopy. *J Cell Biol*. 1975; 67: 911-8
29. **Popescu LM.** Cytochemical study of the intracellular calcium distribution in smooth muscle: surface microvesicles and cellular calcium homeostasis. In: Casteels R. *et al*. eds. Elsevier/North-Holland Biomedical Press, Amsterdam. 1977; pp. 13-23
30. **Popescu LM, Ignat P**. Calmodulin-dependent Ca^{2+} ATPase of human smooth muscle sarcolemma. *Cell Calcium*. 1983; 4: 219-35
31. **Fujimoto T, Nakade S, Miyawaki A, Mikoshiba K, Ogawa K**. Localization of inositol 1,4,5-trisphosphate receptor-like protein in plasmalemmal caveolae. *J Cell Biol*. 1992; 119: 1507-13
32. **Fujimoto T**. Calcium pump of plasma membrane is localized in caveolae. *J Cell Biol*. 1993; 120: 1147-57
33. **Isshiki M, Anderson RGW.** Function of caveolae in Ca^{2+} entry and Ca^{2+}-dependent signal transduction. *Traffic*. 2003; 4: 717-23
34. **Riley M, Baker PN, Tribe RM, Taggart MJ**. Expression of scaffolding, signalling and contractile-filament proteins in human myometria: effects of pregnancy and labour. *J Cell Mol Med*. 2005; 9: 122-34
35. **Gherghiceanu M, Popescu LM**. Caveolar nanospaces in smooth muscle cells. *J Cell Mol Med*. 2006;10: 519-28
36. **Gabella G.** Caveolae intracellulares and sarcoplasmic reticulum in smooth muscle. *J. Cell Sci.* 1971; 8: 601-9
37. **Devine CE, Somlyo AV, Somplyo AP.** Sarcoplasmic reticulum and excitation-contraction coupling in mammalian smooth muscles. *J Cell Biol*. 1972; 52:690–718
38. **Moore ED, Voigt T, Kobayashi YM, Isenberg G, Fay FS, Gallitelli MF, Franzini-Armstrong C**. Organization of Ca^{2+} release units in excitable smooth muscle of the guinea-pig urinary bladder. *Biophys J*. 2004; 87: 1836-47
39. **Franzini-Armstrong C, Protasi F, Ramesh V.** Shape, size, and distribution of Ca^{2+} release units and couplons in skeletal and cardiac muscles. *Biophys J*. 1999; 77: 1528–1539
40. **Ciontea SM, Radu E, Regalia T, Ceafalan L, Cretoiu D, Gherghiceanu M, Braga RI, Malincenco M, Zagrean L, Hinescu ME, Popescu LM**. C-kit immunopositive interstitial cells (Cajal-type) in human myometrium. *J Cell Mol Med*. 2005; 9: 407-20
41. **Popescu LM, Ciontea SM, Cretoiu D, Hinescu ME, Radu E, Ionescu N, Ceausu M, Gherghiceanu M, Braga RI, Vasilescu F, Zagrean L, Ardeleanu C**. Novel type of interstitial cell (Cajal-like) in human fallopian tube. *J Cell Mol Med*. 2005; 9:479-523
42. **Fiala JC**. Reconstruct: a free editor for serial section microscopy. *J Microsc*. 2005; 218: 52-61
43. **Weibel ER.** Stereological Methods. Vol.1: Practical Methods for Biological Morphometry. Academic Press, New York, 1979
44. **Darby PJ, Kwan CY, Daniel EE**. Caveolae from canine airway smooth muscle contain the necessary components for a role in Ca^{2+} handling. *Am J Physiol Lung Cell Mol Physiol*. 2000; 279:L1226-35
45. **Je HD, Gallant C, Leavis PC, Morgan KG**. Caveolin-1 regulates contractility in differentiated vascular smooth muscle. *Am J Physiol Heart Circ Physiol*. 2004; 286:H91-8
46. **Vinten J, Johnsen AH, Roepstorff P, Harpoth J, Tranum-Jensen J**. Identification of a major protein on the cytosolic face of caveolae. *Biochim Biophys Act*a. 2005; 1717: 34–40
47. **Spisni E, Tomasi V, Cestaro A, Tosatto SC**. Structural insights into the function of human caveolin 1. *Biochem Biophys Res Commun*. 2005; 338: 1383–90
48. **Yao Q, Chen J, Cao H, Orth JD, McCaffery JM, Stan RV, McNiven MA**. Caveolin-1 interacts directly with dynamin-2. *J Mol Biol*. 2005; 348: 491–501
49. **Cho WJ, Daniel EE**. Proteins of interstitial cells of Cajal and intestinal smooth muscle, co-localized with Caveolin 1. *Amer J Physiol*. 2005; 288: 571–85
50. **Pelkmans L, Fava E, Grabner H, Habermann B, Krausz E, Zerial M**. Genome-wide analysis of human kinase in clathrin- and caveolae/raft-mediated endocytosis. *Nature* 2005; 436: 78–86
51. **Grilo A, Fernandez ML, Beltran M, Ramirez-Lorca R, Gonzalez MA, Royo JL, Gutierrez-Tous R, Moron FJ, Couto C, Serrano-Rios M, Saez ME, Ruiz A, Real LM**. Genetic analysis of CAV1 gene in hypertension and metabolic syndrome. *Thromb Haemost*. 2006; 95: 696–701
52. **McMahon KA, Zhu M, Know SW, Liu P, Zhao Y, Anderson GW**. Detergent-free caveolae proteome suggests an interaction with ER and mitocondria. *Proteomics* 2006; 6: 143–52
53. **Popescu LM, de Bruijn WC, Diculescu I, Daems WT**. Calcium compartmentalization in skeletal muscle fibers. In: Microbeam Analysis, Wittry DB, ed., San Francisco Press, San Francisco, 1980, pp. 259–64
54. **Morone N, Fujiwara T, Murase K, Kasai RS, Ike H, Yuasa S, Usukura J, Kusumi A.** Three-dimensional reconstruction of the membrane skeleton at the plasma membrane interface by electron tomography. *J Cell Biol*. 2006; 174:851-62
55. **Wamhoff BR, Bowles DK, Owens GK**. Excitation-transcription coupling in arterial smooth muscle. *Circ Res*. 2006; 98:868-78
56. **Popescu LM, de Bruijn WC**. Calcium in the sarcoplasmic reticulum of smooth muscle. X-ray microanalysis of oxalate-treated muscle fibres. Electron Microscopy, vol. 3, Hamburg, 1982, pp. 385-86
57. **Somlyo AV, Gonzalez-Serratos HG, Shuman H, McClellan G, Somlyo AP**. Calcium release and ionic changes in the sarcoplasmic reticulum of tetanized muscle: an electron-probe study. *J Cell Biol*. 1981; 90:577-94

58. **Flynn ER, Bradley KN, Muir TC, McCarron JG**. Functionally separate intracellular Ca^{2+} stores in smooth muscle. *J Biol Chem*. 2001; 276:36411-8
59. **McGeown JG**. Interactions between inositol 1,4,5-trisphosphate receptors and ryanodine receptors in smooth muscle: one store or two? *Cell Calcium.* 2004; 35:613-9
60. **Poburko D, Kuo KH, Dai J, Lee CH, Van Breemen C.** Organellar junctions promote targeted Ca^{2+} signaling in smooth muscle: why two membranes are better than one. *Trends Pharmacol Sci.* 2004; 25: 8-15
61. **Michelangeli F, Ogunbayo OA, Wooton LL.** A plethora of interacting organellar Ca^{2+} stores. *Curr Opin Cell Biol*. 2005; 17:135-140
62. **Fameli N, Van Breemen C, Kuo KH.** A quantitative model for refilling of the sarcoplasmic reticulum during vascular smooth muscle asynchronous [Ca^{2+}] oscillations. *http://arxiv.org/abs/q-bio/0603001* 2006
63. **Davidson SM, Duchen MR**. Calcium microdomains and oxidative stress. *Cell Calcium*. 2006; 40: 561-74
64. **Filippin L, Magalha es PJ, Di Benedetto G, Colella M, Pozzan T.** Stable interactions between mitochondria and endoplasmic reticulum allow rapid accumulation of calcium in a subpopulation of mitochondria. *J Biol Chem*. 2003; 278:39224–39234
65. **Jacobson J, Duchen MR.** Interplay between mitochondria and cellular calcium signalling. *Mol Cell Biochem*. 2004; 256-257:209-18
66. **Alonso MT, Villalobos C, Chamero P, Alvarez J, Garcia-Sancho J.** Calcium microdomains in mitochondria and nucleus. *Cell Calcium*. 2006; 40:513-25
67. **Csordas G, Renken C, Varnai P, Walter L, Weaver D, Buttle KF, Balla T, Mannella CA, Hajnoczky G.** Structural and functional features and significance of the physical linkage between ER and mitochondria. *J Cell Biol*. 2006; 174:915-21
68. **Jaeger J, Reinitz J.** On the dynamic nature of positional information. *BioEssays*. 2006; 28:1102–1111